THREE-DIMENSIONAL DISTANCE BASED GEOSTATISTICAL MODELS TO ADJUST RADAR RAINFALL DATA

A Thesis

Presented to

the Faculty of the Department of Civil and Environmental Engineering

University of Houston

In Partial Fulfillment of the

Requirements for the Degree Master of Science in

Civil Engineering

by

Erkan KARAKOYUN

May 2016

THREE-DIMENSIONAL DISTANCE BASED GEOSTATISTICAL MODELS TO ADJUST RADAR RAINFALL DATA

Erkan Karakoyun

Approved:

Chair of the Committee
Keh-Han Wang, Professor
Civil and Environmental Engineering

Committee Members:

Yi-Lung Mo, Professor
Civil and Environmental Engineering

Hyongki Lee, Assistant Professor
Civil and Environmental Engineering
Geosensing Systems Engineering and Science

Ted Chu, PhD, PE, CFM
Project Engineer, Water
AECOM

Suresh K, Khator, Associate Dean
Cullen College of Engineering

Roberto Ballarini, Professor and Chair
Civil and Environmental Engineering

ACKNOWLEDGEMENTS

I would like to thank Dr. Wang for accepting me as his student, helping and encouraging me for this study. His patience and guidance always help me to find the right way. I also want to thank Dr. Ted Chu for kindly helping me whenever I had questions. I have been lucky to have this kind of kindly people to overcome problems and finish this study.

I would like to thank the Turkish Ministry of Education for financially supporting me and giving me a chance to make my dream come true.

Lastly to my lovely wife Tuba with my deepest gratitude. Her support and encourage always kept me standing up. Also, my son Halis Emre and my little daughter Elif Betul for motivating me against the problems with even only their presence. Also thank to my parents, sister and brother for their support and making me feel like at home.

THREE-DIMENSIONAL DISTANCE BASED GEOSTATISTICAL MODELS TO ADJUST RADAR RAINFALL DATA

An abstract

of a

Thesis

Presented to

The Faculty of the Department of Civil and Environmental Engineering

University of Houston

In Partial Fulfillment of the

Requirements for the Degree Master of Science in

Civil Engineering

by

Erkan KARAKOYUN

May 2016

ABSTRACT

Accurate and reliable rainfall input is crucial for hydrological modeling studies. Rain gauge collection and weather radar rainfall estimate are two of the most common techniques used for receiving rainfall data at a watershed. This study focuses on the development of three-dimensional (3D) distances based geostatistical models, such as Regression Kriging (RK) and Merging methods, to perform the adjustments of radar rainfall data to the targeted gauge measurements. These models are tested at the Chenyulan River watershed using the rainfall events of five typhoons landed Taiwan in recent years. Two-dimensional (2D) distance based models are also simulated to compare the adjusted rainfall values with those from 3D distance approaches. Results from Ordinary Kriging (OK) and gauge data are also included for comparisons. It is found in general the radar rainfall data can be corrected more accurately using the developed RK or Merging models than OK. Additionally, the adjusted rainfall values from 3D distance based models are similar to those using 2D distance based calculations at most tested stations. Depending on the typhoon events, using 3D distances in the semivariogram and Kriging interpolations is shown to be able to produce improved estimations of radar rainfall rates than 2D distance based calculations.

TABLE OF CONTENTS

ACKNOWLEDGEMENTS .... **v**

ABSTRACT .... **vii**

TABLE OF CONTENTS .... **viii**

LIST OF FIGURES .... **x**

LIST OF TABLES .... **xi**

NOMENCLATURE .... **xii**

1 Introduction **1**

1.1 Overview 1

1.2 Research Goals 3

1.3 Contents of Study 4

2 Literature Review **5**

2.1 Review of Previous Studies 5

2.2 Research Significance 8

3 Study Area **9**

3.1 Overview of the Study Area 9

3.2 Historical typhoon events 11

4 Rainfall Data **16**

4.1 Rain Gauge Obsevations 16

4.2 Radar Rainfall Estimates 19

5 Geostatistical Based Interpolation Methods 21

5.1 Regression Kriging Method 21

5.2 Merging Method 25

6 Results 27

6.1 Typhoon Kalmaegi 28

6.2 Typhoon Morakot 39

6.3 Typhoon Fungwong 48

6.4 Typhoon Sinlaku and Typhoon Fanapi 55

7 Conclusions and Recommendations for Future Studies 62

REFERENCES 65

LIST OF FIGURES

Figure 1.1. Landslide in Taiwan caused by typhoon Morakot 2
Figure 3.1. Location of Chenyulan watershed. 9
Figure 3.2. Typhoon Kalmaegi travel path, photo courtesy of CWB 13
Figure 3.3. Typhoon Fungwong travel path, photo courtesy of CWB 13
Figure 3.4. Typhoon Sinlaku travel path, photo courtesy of CWB 14
Figure 3.5. Typhoon Morakot travel path, photo courtesy of CWB 14
Figure 3.6 Typhoon Fanapi travel path, photo courtesy of CWB................................... 15
Figure 4.1 Rain gauges location on watershed 18
Figure 4.2. The radar coverage of Taiwan, photo courtesy of CWB 20
Figure 5.1. Sample 2D Semivariogram for typhoon Kalmaegi 24
Figure 5.2. Sample 3D Semivariogram for typhoon Kalmaegi 25
Figure 6.1. Improvements by RK, Merging and OK method with 2D and 3D distance for Typhoon Kalmaegi.. 32
Figure 6.2. Improvement differences between 2D and 3D rain gauge distance for Typhoon Kalmaegi.. 33
Figure 6.3. Peak hour comparison by using 2D distance for Typhoon Kalmaegi 35
Figure 6.4. Peak hour comparison by using 3D distance for Typhoon Kalmaegi 36
Figure 6.5. Adjusted Rainfall Rate using 2D distance versus Unadjusted Rainfall Rate obtained from Rain Gauges for typhoon Kalmaegi 37
Figure 6.6. Adjusted Rainfall Rate using 3D distance versus Unadjusted Rainfall Rate obtained from Rain Gauges for typhoon Kalmaegi 38
Figure 6.7. Improvements by RK, Merging and OK by 2D and 3D distance for Typhoon Morakot.. 42
Figure 6.8. Improvement differences between 2D and 3D rain gauge distance for Typhoon Morakot. 43
Figure 6.9. Peak hour comparison by using 2D distance for Typhoon Morakot............. 44
Figure 6.10. Peak hour comparison by using 3D distance for Typhoon Morakot............ 45
Figure 6.11. Adjusted Rainfall Rate using 2D distance versus Unadjusted Rainfall Rate obtained from Rain Gauges for typhoon Morakot.. 46
Figure 6.12. Adjusted Rainfall Rate using 3D distance versus Unadjusted Rainfall Rate obtained from Rain Gauges for typhoon Morakot.. 47
Figure 6.13. Improvements by RK, Merging and OK by 2D and 3D distance for Typhoon Fungwong 51
Figure 6.14. Improvement differences between 2D and 3D rain gauge distance for Typhoon Fungwong.. 52
Figure 6.15. Peak hour comparison by using 2D distance for Typhoon Fungwong 53
Figure 6.16. Peak hour comparison by using 3D distance for Typhoon Fungwong 54
Figure 6.17.Improvements by RK, Merging and OK by 2D and 3D distance for Typhoon Sinlaku 58
Figure 6.18. Improvements by RK, Merging and OK by 2D and 3D distance for Typhoon Sinlaku 59
Figure 6.19. Peak hour comparison by using 2D distance for Typhoon Sinlaku. 60
Figure 6.20. Peak hour comparison by using 2D distance for Typhoon Sinlaku. 61

LIST OF TABLES

Table 3.1. Elevation distribution of Chenyulan watershed 10
Table 3.2. Slope distribution of Chenyulan river watershed 11
Table 3.3. Summaries of five typhoons 12
Table 4.1. Rain Gauge Stations... 17
Table 6.1.RMSE analysis based on RK, Merge and OK by using 2D and 3D distance for Typhoon Kalmaegi.. 31
Table 6.2. RMSE analysis based on RK, Merge and OK by using 2D and 3D distance for Typhoon Morakot 40
Table 6.3. RMSE analysis based on RK, Merge and OK by using 2D and 3D distance for Typhoon Fungwong 50
Table 6.4. RMSE analysis based on RK, Merge and OK by using 2D and 3D distance for Typhoon Sinlaku.. 56
Table 6.5. RMSE analysis based on RK, Merge and OK by using 2D and 3D distance for Typhoon Fanapi 57

NOMENCLATURE

Z	Radar Reflectivity for *Z-R* relationship
R	Rainfall Rate for *Z-R* relationship
a	Coefficient of *Z-R* relationship
b	Coefficient of *Z-R* relationship
β_a	Regression coefficient
β_0	Intercept of regression line
$\vec{x}_i$	The position vector of the *i*th gauge station
$P_g\vec{x}_i$	Rain gauge observation at $\vec{x}_i$
m	Total number of predictors for regression analysis
$g_a(\vec{x}_i)$	Auxiliary variable
$\varepsilon(\vec{x}_i)$	Residual at $\vec{x}_i$
n	Total number of gauge station
$R(\vec{x}_i)$	Radar rainfall rate at $\vec{x}_i$
$E(\vec{x}_i)$	Elevation at $\vec{x}_i$
$\vec{x}_p$	The position vector of ungauged locations
$\varepsilon(\vec{x}_p)$	Residuals at $\vec{x}_p$
ω_{ip}	Kriging weight at x_i with respect to $\vec{x}_p$
$\gamma(h)$	Semivariance for gauge separation distance of h
$n(h)$	Number of pairs of residuals separated by h
$\varepsilon(\overrightarrow{x_\iota + h})$	Residuals further from $\varepsilon(\vec{x}_i)$ by a distance h
μ	Lagrange multiplier
$\Delta R(\vec{x}_p)$	Adjustments at $\vec{x}_p$
$R_r(\vec{x}_p)$	Unadjusted radar rainfall rate at $\vec{x}_p$
$R_r(\vec{x}_i)$	Unadjusted radar rainfall rate at $\vec{x}_i$
$R(\vec{x}_p)$	Final rainfall rate at $\vec{x}_p$
$RMSE(\vec{x}_i)$	Root mean square error at $\vec{x}_i$

$R_t(\vec{x}_i)$	Adjusted rainfall rate at $\vec{x}_i$an time t
$R_{gt}(\vec{x}_i)$	Observed gauge measurement at $\vec{x}_i$and time t
t	time

1 Introduction

1.1 Overview

Water is one of the most important natural resources in the Earth and Hydrology is the science that provides the knowledge of the distribution, movement, availability and quality of water hydraulic within each stage of hydrologic or water cycle. Undoubtedly rainfall is the most important input of water cycle. Also rainfall recording and measurements are crucial for the study of hydrological and hydraulic systems. Issued related to the design of hydraulic structures, such as dam, channels, canals, spillways etc. flood prediction, soil erosion and urbanization depend on the rainfall intensity. All the indicated studies require accurate measurements of the rainfall intensity within the event duration (Knight et al., 2005). In addition, the rainfall caused natural hazards such as typhoons, floods, land slices are increasing (Pielke & Downton, 2000). As a result early prediction of flooding using the inputs of rainfall data becomes practically more important.

On average, 3.5 typhoons strike Taiwan every year since it is located on the path of typhoons in northwest Pacific (Chen et al., 2013). Typhoon Morakot in August 2009 is the deadliest typhoon to impact Taiwan in recorded history. It caused 461 death and 192 missing people. It brought tremendous rainfall over Taiwan and that triggered mudflow. Figure 1.1 shows a massive mudflow caused by Typhoon Morakot. Another impact of Morakot was agricultural loses and tourism industry so the total damage is reached 3.3 billion USD (Chen et al., 2013).

Figure 1.1. Landslide in Taiwan caused by typhoon Morakot

The rainfall measurements obtained from rain gauges are able to provide accurate and reliable results in specific locations, but gauging stations cannot effectively account for the spatial variability of precipitation. Because of this, in order to get spatial rainfall distribution at the ungauged locations spatial interpolation methods are required such as Thiessen polygon techniques (Thiessen, 1911) and inverse distance weighted (IDW). In addition, geostatistical methods, such as Kriging, can in general provide more accurate spatial prediction (Prudhomme & Reed, 1999). Kriging uses a semivariogram to assess spatial correlation between rainfall data. In this study the three-dimensional (3D) true distance instead of the two-dimensional (2D) distance, which is commonly used, is applied in semivariogram for the application of Kriging method for rainfall estimations.

Data collected with rain gauge have been the traditional and most commonly used techniques to obtain the rainfall information in the past. However, recently weather radar has also been widely utilized to predict rainfall data. Radar rainfall data can capture the spatial variability of rainfall fields and map spatial variability of rainfall more accurately. Also, it is an effective way for obtaining rainfall field with better spatial and temporal resolution covering a large area (Hanchoowong et al., 2012). However, rainfall data obtained from only radar cannot be used directly due to uncounted error from radar signals. The principle of radar rainfall measurement is based on the amount of energy scattered back from rain above the ground surface. For the reasons of data corrections, radar rainfall estimates require to be merged with rain gauge observations which are commonly thought as ground truth measurements, for more accurate and reliable prediction of rain fields.

1.2 Research Goals

As discussed earlier rainfall input is the most critical variable in hydrological simulation. Thus, obtaining accurate rainfall data would become extremely important. In this study rainfall data obtained from rain gauges which are known more accurate and radar conversions are merged together to improve the radar predictions. Spatial interpolation techniques such as Regression Kriging (RK) and Merging method (Merge) are used and coded with R statistical programming language to develop the correction procedure.

Rain gauges are ground based instruments. In Kriging interpolation method, distance based semivariogram can be obtained to develop correlations for the data between rain gauges. Commonly 2D distance is issued while computing the distance of rain gauges for the development of semivariogram. However, depending on the terrain of the watershed, rain gauges may be placed at sites of different elevation. Then, the true 3D distance can potentially be utilized to improve the representation of semivariogram. The principle aim of this study is to examine the prediction accuracy of rainfall data by applying the spatial interpolation techniques, RK and Merging, with the use of 2D and 3D distance of rain gauges. The results from 2D and 3D distance associated calculations and gauge data are compared. Rainfall data from five historical typhoons, Morakot, Kalmaegi, Sinlaku, Fanapi and Fungwong, hit Taiwan are used for testing the models and results comparisons.

1.3 Contents of Study

This thesis has seven chapters. In the first chapter introduction is given with the aim of this study. Chapter 2 represent a literature review of previous studies on related with this study. The study area of this thesis explained in Chapter 3. After explanation of study area Chapter 4 gave how to obtained rainfall data. Chapter 5 presents the spatial interpolation methods, RK and Merging that used in this study. Chapter 6 presents and compare the results of the interpolation methods with using 2D and 3D distance between rain gauges. Lastly, Chapter 7 presents conclusion and recommendation for future studies.

2 Literature Review

2.1 Review of Previous Studies

It is common agreement by many researchers that rainfall input is the most important variable for hydrological simulation and its application, such as flash flood forecasting (Gooverts, 2000; Goudenhoofdt & Delobbe, 2009; Lopez, Napolitano & Russo, 2005; Chen & Liu, 2012; Cole & Moore, 2008; Berne & Krajewski, 2013), channel improvement etc. Because of the essential importance of the rainfall data for the watershed modeling, the rainfall measurement should be accurate and reliable.

Rain gauge data are commonly thought as true measurements over a small area (Delrieu et al, 2014; Wardah et al, 2011). However, the small scale of measurements at limited gauge stations tends to biases on prediction for rainfall over the whole basin (Delrieu et al., 2014; Lopez, Napolitano & Russo, 2005). Utilizing radar rainfall data, which cover a large area of targeted watershed, in hydrological modeling have been investigated by many researches in recent years (Goudenhoofdt & Delobbe, 2009; Chumchean et al., 2006; Forero et al., 2009). Weather radar estimations in terms of rainfall values have some advantages than rain gauge observations. Radar can provide rainfall data in a very large area with high temporal and spatial distribution (Lopez et al., 2005). However, due to the uncertainty of radar data, the accuracy and spatial variability of rain fields are generally required calibration using the rain gauge measurements (Goudenhoofdt & Delobbe, 2009).

As discussed earlier, rainfall obtained from rain gauges or radar reflectivities are two most frequently used instruments for measurements. However, rain gauges due to their scattered distribution may introduce the deficiency in hydrological modeling process. The low density and irregular locations of rain gauges are generally not able to cover large spatial area of rain fields. For this consideration, weather radar estimation would help to overcome the site limiting issue, since radar can provide indirect reflectivities of large area rain fields with fine distribution in time and space. Cole and Moore (2008) found that gauge adjusted radar data demonstrate a better estimation than only using originally unadjusted radar data. Combining rain gauge measurements and radar rainfall estimates have been used to obtain more accurate rainfall values since the beginning of the use of weather radars in the 70`s (Goudenhoofdt & Delobbe, 2009).

Since radar measures reflectivity caused by rainfall intensity to predict the rainfall distribution at covered areas, sources of error, such as Z-R conversion error and reflectivity measurement error affect the accuracy of rainfall estimations. (Hanchoowong et al., 2012; Borga, 2002; Lopez et al., 2005). Here, Z represent rainfall intensity and R denotes the radar reflectivity. Reflectivity factor converted to rainfall rates commonly uses the Marshall-Palmer relation $Z = aR^b$ (Goudenhoofdt & Delobbe, 2009). Joss & Lee (1995), Chumchean et al. (2004) and Chumchean et al. (2008) investigated the methodologies to reduce those errors. Also, Gjertsen, Salek & Michelson (2003) reported that the application of gauge adjustment could correct not only the inaccurate Z-R relationship but also the radar errors such as the distance caused attenuation in precipitation. They indicated that the initial Z-R relationship is not that critical when the adjustment of gauge data are applied to the radar estimations.

Interpolation methods such as Thiessen polygon method (Thiessen, 1951) and Inverse Distance Weighted (IDW) method have been used to obtain rainfall data at ungauged locations. These conventional methods sometimes become insufficient and the interpolated results are not that accurate due to the lack of rain gauge density. Especially in the mountain area the cost of placing rain gauges and maintaining the functionality of the gauges are very high (Sarangi, Cox & Madramootoo, 2005). To improve the rainfall estimations, geostatistical methods such as Kriging can overcome the problems of less accurate interpolation methods. Since Kriging method uses the spatial correlation between neighboring points to predict attribute values at ungauged locations (Gooverts, 2000; Sarangi, Cox & Madramootoo, 2005). Gooverts (2000), Tabios & Salas (1985), Philips et al. (1992) and Delbari & Afrasiab (2013) concluded that geostatistical method, Kriging, gave a better prediction of rainfall data than conventional methods, such as Thiessen and IDW.

RK is a incorporated method that associated the prediction provided from regression considering spatial correlation and the residual predicted from the OK (Teng et al. (2014). The researchers Hengl et al. (2004) and Sun et al. (2012) concluded that RK gives more accurate prediction than OK.

Rain gauge observation is commonly regarded more accurate to measure rainfall but it is limited to spatial significance. Radar rainfall data can capture the spatial variability of rainfall fields and map spatial variability of rainfall more accurately but it has error. Due to both methods have some deficiency many researchers Ehret (2003), Gooverts (2000), combine the rain gauge data with radar data to estimate the more accurate rainfall. In some studies (Ehret 2003, Chu 2014) Merging method used as a spatial interpolation method to predict rainfall and they concluded that Merging method produce reasonably well results.

Chu (2014) also concluded that the multivariate techniques such as RK and Merging are able to reasonably correct the raw radar rainfall data values to close to the gauge measurements. He also demonstrated that although RK and Merging methods utilize different spatial interpolation procedure both methods are shown similar results in terms of the interpolated radar rainfall values. In addition to the RK and Merging methods he concluded that RK and Merging methods can produce better improved radar rainfall data than the univariate method OK.

2.2 Research Significance

Radar rainfall could be adjusted by using rain gauge measurements and radar rainfall estimates utilizing some interpolation methods. Several studies are available for this estimation mentioned above, however this study aimed to investigate to predict and adjust the rainfall with using 3D real distance between rain gauges in geostatistical methods as conversely common used 2D distance.

3 Study Area

3.1 Overview of the Study Area

In this research, Chenyulan river watershed in Taiwan is selected as the study area. It is located in Nantou County of central Taiwan. The total area of watershed is nearly 450 km^2. Figure 3.1 shows the location of the watershed. The watershed area is mostly mountainous. The average elevation is 1580 meters and only 3.1 percent of total area are lower than 500 meters. The elevation distribution is shown in Table 3.1.

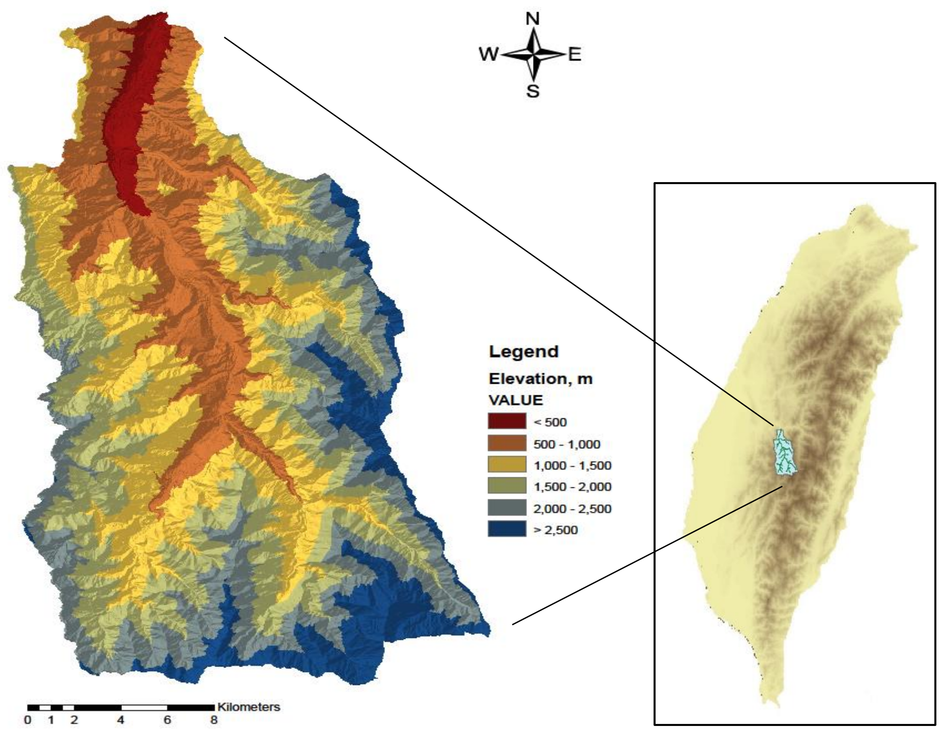

Figure 3.1. Location of Chenyulan watershed.

The annual rainfall is between 2000 mm and 5000 mm with the average 3500 mm in the watershed. The rainy season is between May to October and nearly 80 % of annual rainfall occur in this time period especially during typhoon events which is generally hit Taiwan three or four times a year (Chen et al., 2013).

Table 3.1. Elevation distribution of Chenyulan watershed

Elevation (m)	**Area (km^2)**	**Percentage (%)**
< 500	13.8	3.1
500 – 1000	88.6	19.9
1000 – 1500	110.4	24.8
1500 – 2000	105.5	23.7
2000 – 2500	80.2	18
2500 – 3000	36.5	8.2
>3000	10.2	2.3
Total	**445.3**	**100**

Mount Yushan is located in the south of the watershed where the elevation is more than 3000 meters and descends to the north where the elevation is around 300 meters. The Chenyulan river with the length of 42 kilometers flows from south to north. The river is relatively steep with the average slope of 6.75%. For the watershed, the average slope of the Chenyulan river basin is nearly 36 degrees and only an approximately 17% of the total area has a slope less than 20 degrees which means it is highly possible for flash flood risk. Table 3.2 shows the slope distribution of Chenyulan river watershed.

Table 3.2. Slope distribution of Chenyulan river watershed

Slope (degree)	Area (km^2)	Percentage (%)
0 -10	32.1	7.2
10 – 20	42.6	9.6
20 – 30	100.4	22.6
30 – 40	161.9	36.4
>40	108.8	24.3
Total	**445.3**	**100**

3.2 Historical typhoon events

In this study the rainfall data were selected from five typhoon events (Kalmaegi, Fungwong, Sinlaku, Morakot and Fanapi) which hit the Taiwan from 2008 to 2010. Table 3.3 shows the details of the five typhoon events, including the total rainfall depth. Even though four typhoons classified as a category moderate with Sinlaku as a category strong, they produced substantially different results since each typhoon had its own traveling path, speed and rainfall amount carried. The travelling paths of the five typhoons mentioned above are shown in Figures 3.2 – 3.6 (http://rdc28.cwb.gov.tw/TDB/ntdb/pageControl/ty_warning).

Table 3.3. Summaries of five typhoons

Name	Strength	Duration	Rainfall (mm)	Speed (mph)
Kalmaegi	Moderate	07/16/2008 – 07/18/2008	766	104
Fungwong	Moderate	07/26/2008 – 07/29/2008	816	109
Sinlaku	Strong	09/11/2008 – 09/16/2008	1485	144
Morakot	Moderate	08/05/2009 – 08/10/2009	2880	92
Fanapi	Moderate	09/17/2010 – 09/20/2010	305	105

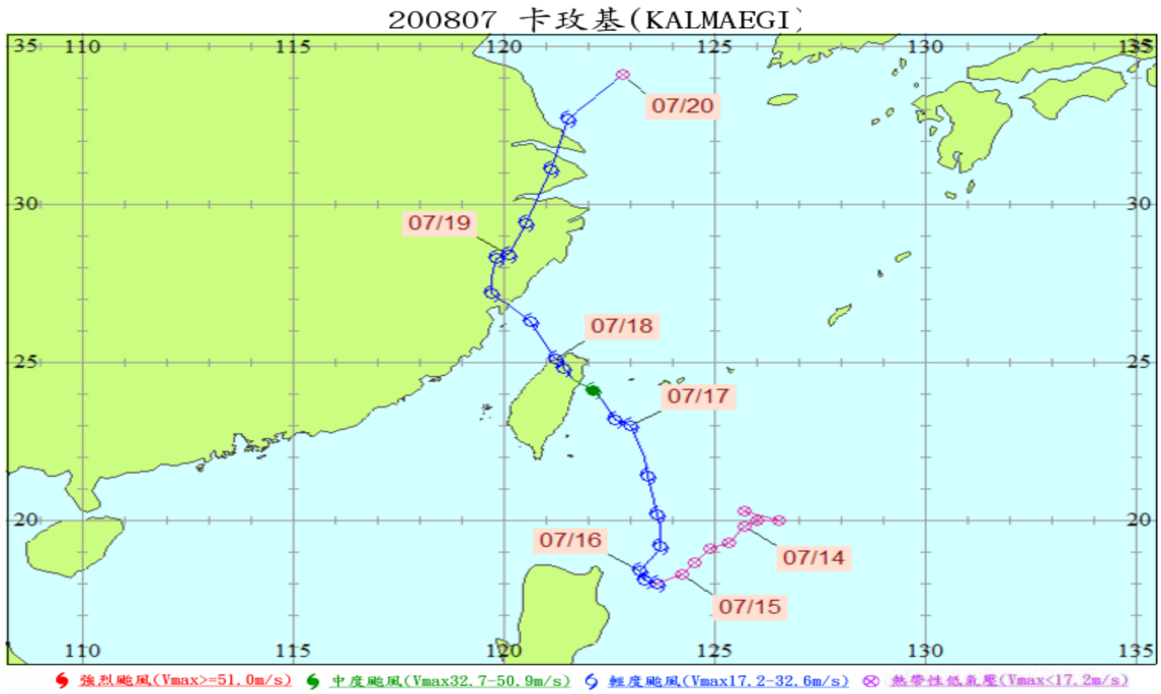

Figure 3.2. Typhoon Kalmaegi travel path, photo courtesy of CWB

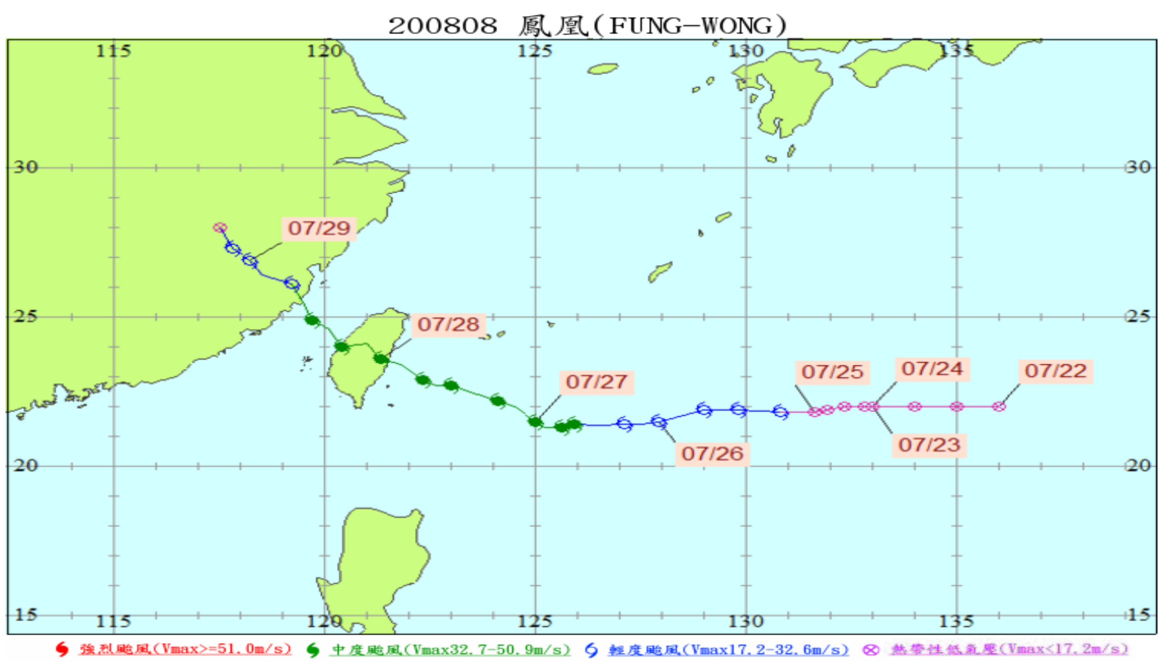

Figure 3.3. Typhoon Fungwong travel path, photo courtesy of CWB

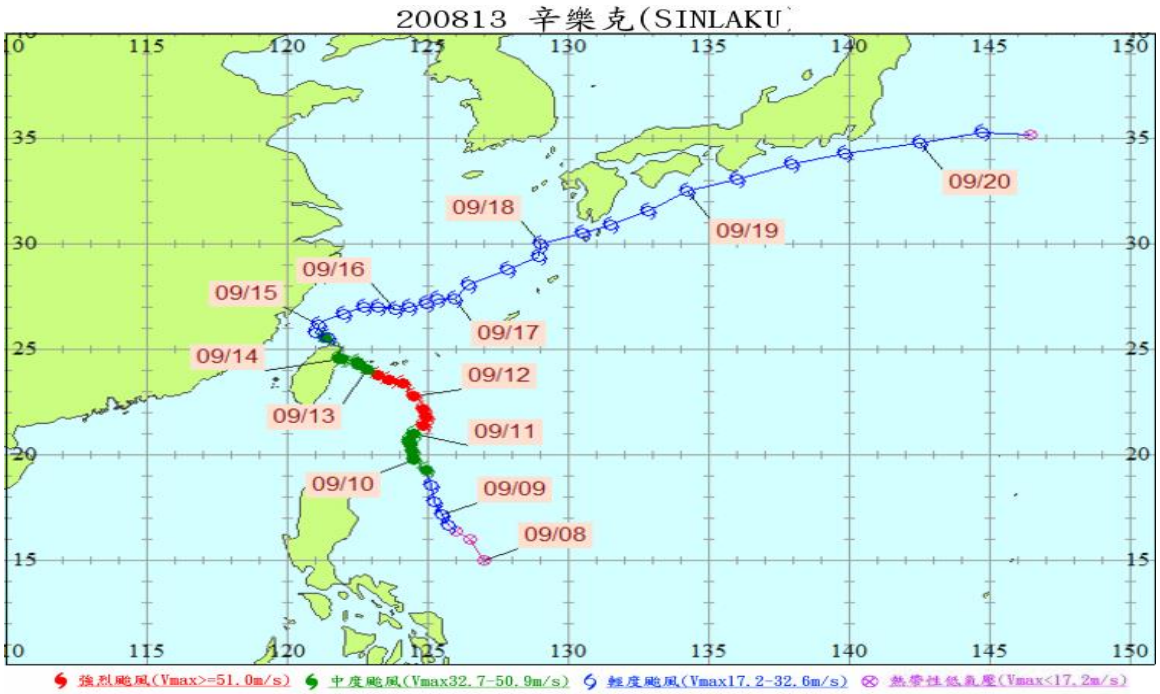

Figure 3.4. Typhoon Sinlaku travel path, photo courtesy of CWB

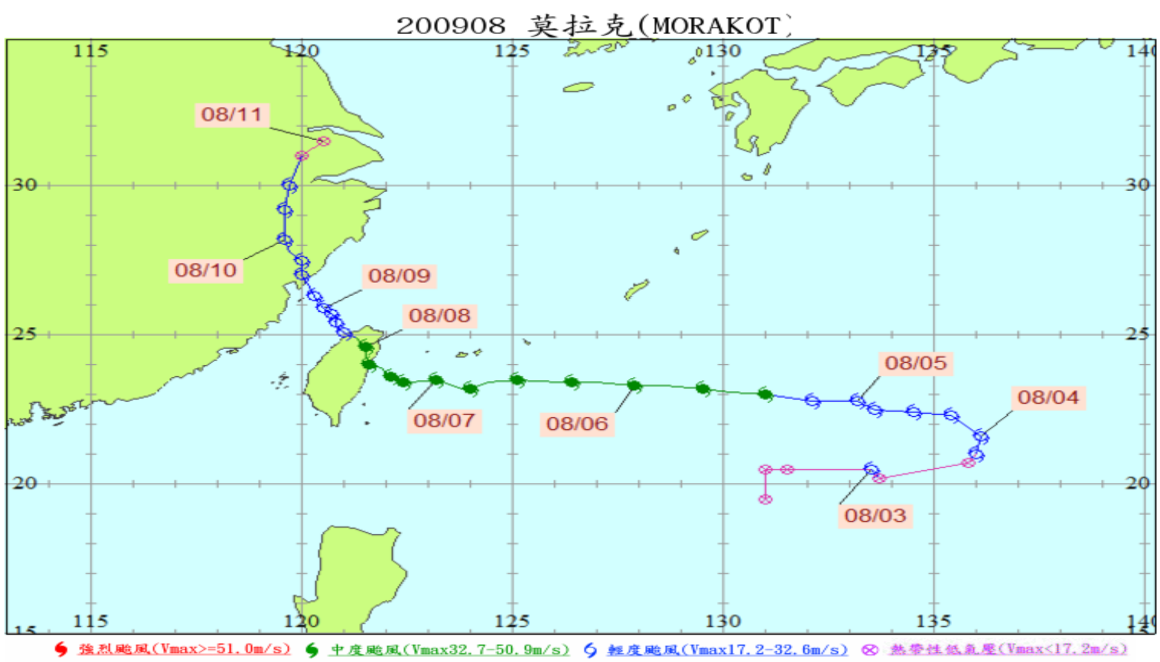

Figure 3.5. Typhoon Morakot travel path, photo courtesy of CWB

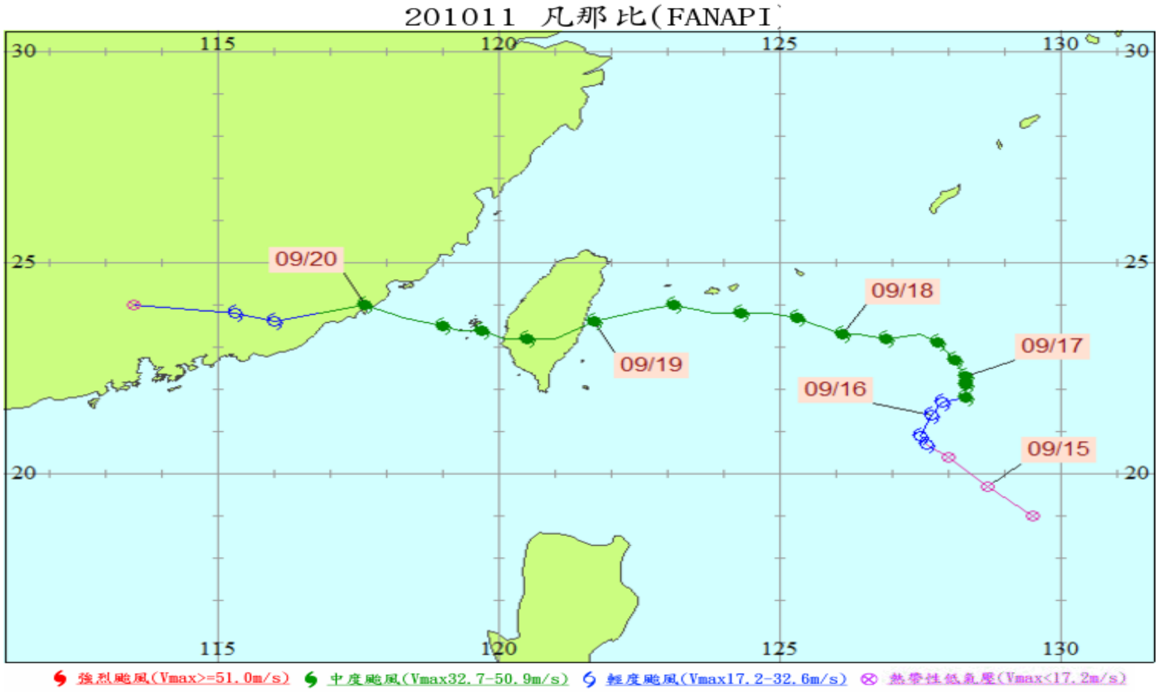

Figure 3.6 Typhoon Fanapi travel path, photo courtesy of CWB

4 Rainfall Data

In this study, rain gauge data and radar rainfall estimations are combined to perform interpolation. These two of rainfall data measurements are described in more detail in the following sections.

4.1 Rain Gauge Obsevations

The rain gauge observations provided by the Central Weather Bureau (CWB) of Taiwan and Water Resources Agency (WRA) were adopted for this study. Among 27 rain gauge stations, 23 rain gauges are managed by CWB while 4 stations are monitored by WRA. The details of rain gauge locations and associated vertical elevations of the watershed are shown in Figure 4.1 and Table 4.1.

Table 4.1. Rain Gauge Stations

Stations ID	X (m)	Y (m)	Elevation (m)
C1I270	234294	2636644	593
C1I150	243999	2632976	393
C1I160	236100	2630859	399
C1I310	237315	2628059	1001
C1I300	236321	2625168	781
C1I090	227485	2625117	878
C1I100	229513	2617731	1771
C1I120	224672	2619646	1528
C1I290	237646	2618491	1151
C1I080	233965	2620864	536
C1I060	240079	2613075	1181
C1I070	237837	2609909	825
C1I340	235680	2606957	897
C1I350	241492	2606092	887
C0H9A0	233124	2603669	1595
C1V460	238192	2592805	1949
C1M440	236749	2597543	2540
C1V170	244494	2595785	3690
C1M630	223550	2610420	1052
467550	245063	2598461	3845
467530	230086	2600812	2413
C1I170	226257	2636040	235
C1I040	251302	2635836	1693
1510P088	240775	2623180	1666
1510P087	241806	2613068	2200
1510P030	241857	2606708	1135
1510P132	233702	2596708	2540

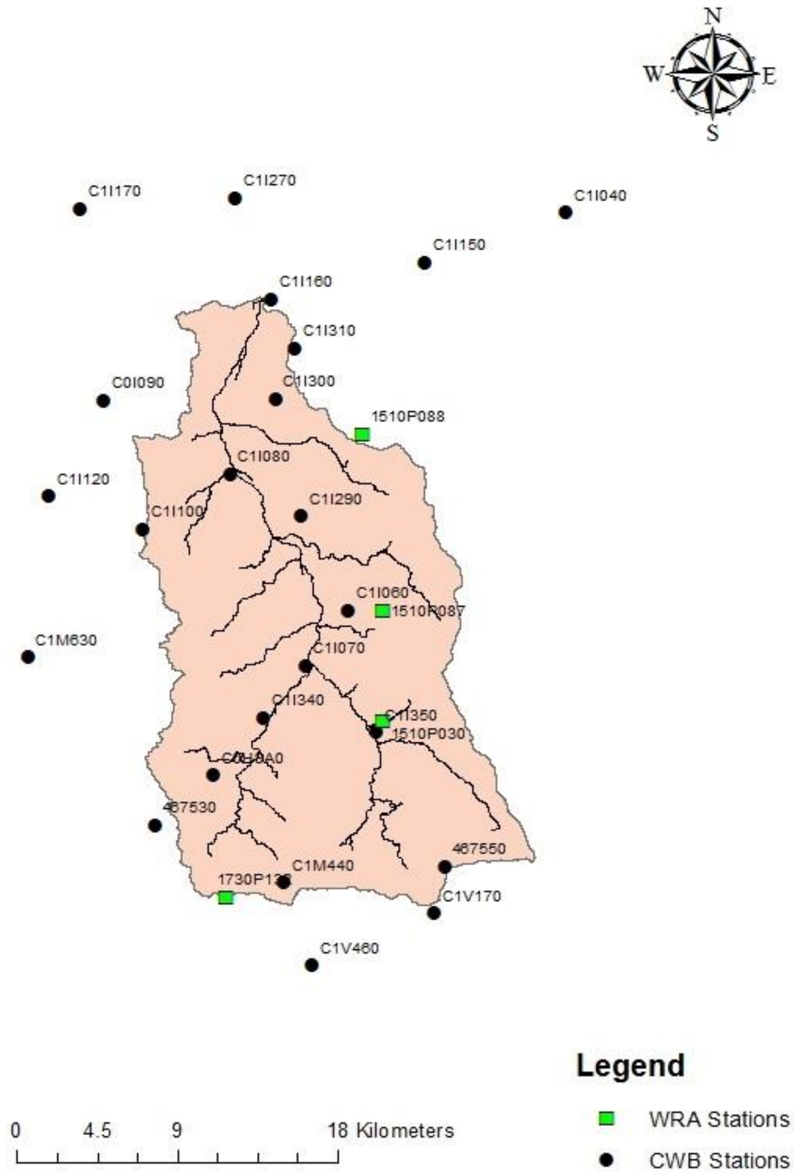

Figure 4.1 Rain gauges location on watershed

4.2 Radar Rainfall Estimates

The raw radar rainfall data obtained are based on the Quantitative Precipitation Estimation and Segregation Using Multiple Sensors (QPESUMS) system. The QPESUMS system were jointly developed by the agencies of CWB, WRA, and Soil and Water Conservation Bureau (SWCB) in Taiwan and the National Severe Storms Laboratory (NSSL) of US in 2002 to utilize radar systems for rainfall data collection and improve the monitoring of severe weather. After QPESUMS put into operation, it has been used to provide rainfall observations, such as 1 – 72 hours rainfall data, 0 - 1 hour precipitation forecast, real time lighting reporting and 0 – 1 hour storm probability.

QPESUMS system utilize weather radar data for rainfall estimations. Figure 4.2 shows the radar stations in Taiwan. The radar rainfall approximated from the scanned data follows the *Z*-*R* relationship through the QPESUMS system as

$$Z = aR^b, \tag{4.1}$$

where *Z* is radar reflectivity (dBZ) and *R* is rainfall rate (mm/hr) and the coefficient *a* and the component *b* are derived constants. The *Z*-*R* relationship in general is different from place to place and depends on the precipitation type. For the use in Taiwan, the CWB of Taiwan found the coefficient *a* and the component *b* are respectively 32.5 and 1.65.Then, Equation (4.1) becomes

$$Z = 32.5R^{1.65}. \tag{4.2}$$

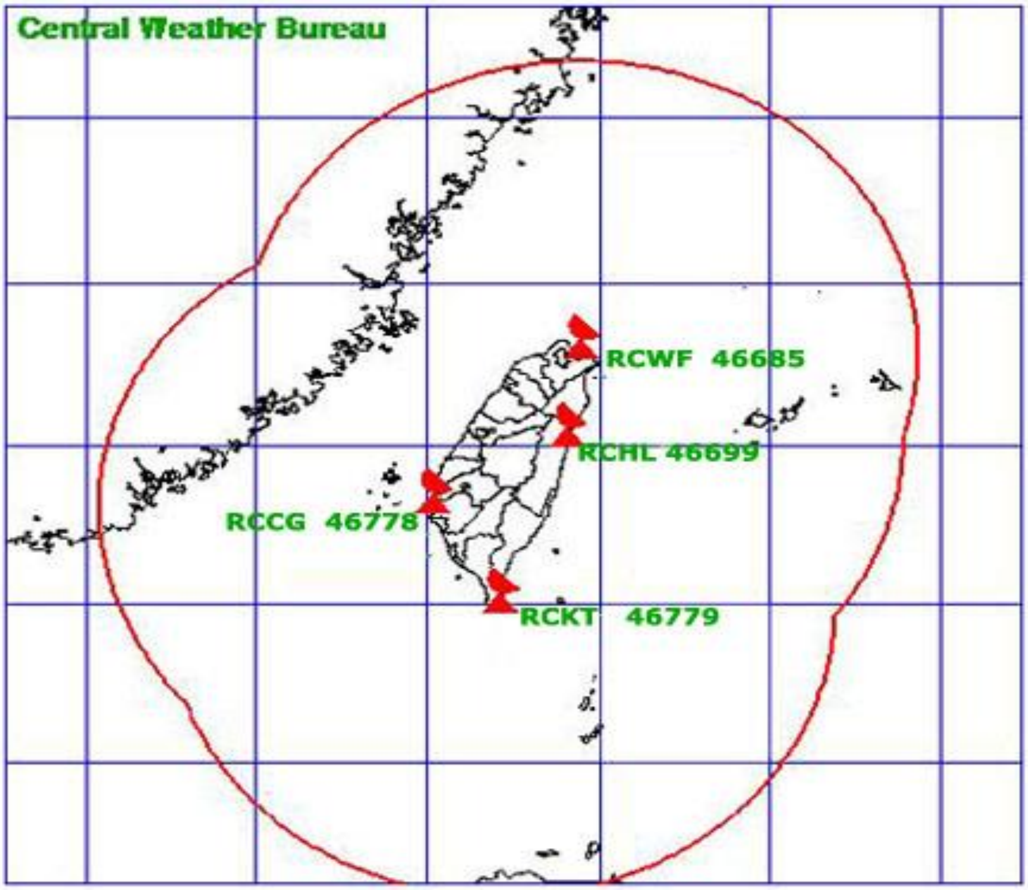

Figure 4.2. The radar coverage of Taiwan, photo courtesy of CWB

The radar rainfall data obtained from CWB are stored in grid format which is 1.25 km x 1.25 km cell size and the recording interval is 10 minutes.

5 Geostatistical Based Interpolation Methods

In this study, two geostatistical based interpolation methods namely Regression Kriging (RK) and Merging methods, are applied to improve the accuracy of the new radar rainfall data.

5.1 Regression Kriging Method

Regression Kriging (RK) approach is adopted as one of the spatial interpolating methods in this study to improve the adjustment of the radar rainfall data. The RK includes the deterministic (regression, trend) and stochastic (kriging, residuals) procedures for the data adjustments. Linear regression is generally utilized for the deterministic part. The rainfall data from gauge stations are considered as the target variable while the radar data extracted from the QPESUMS system are used as the inputs of auxiliary variables in regression analysis of the present study. The stochastic part which distributes the residuals is based on the Kriging interpolation procedure. Overall, the RK rainfall values are obtained by summing the regression values and residuals.

The linear regression analysis of multiple variables has the following equation

$$P_g(\vec{x}_i) = \beta_0 + \sum_{a=1}^{m} \beta_a g_a(\vec{x}_i) + \varepsilon(\vec{x}_i) \quad i = 1,2,3,\ldots..n, \qquad (5.1)$$

where β_a are the regression coefficient, β_0 is the intercept, $\vec{x}_i = (x_i, y_i)$, the position vector of the ith gauge station, P_g is the gauge rainfall observation, m is the total number of predictors (auxiliary variables), g_a $(a=1,2,\ldots m)$ is the auxiliary variables, ε is the residuals, n is the total number of gauge stations. Considering the radar data $R(\vec{x}_i)$ and elevation $E(\overrightarrow{x_i})$ as the auxiliary variables, the Equation (5.1) becomes

$$P_g(\vec{x}_i) = \beta_o + \beta_1 R(\vec{x}_i) + \beta_2 E(\vec{x}_i) + \varepsilon(\vec{x}_i)\ . \tag{5.2}$$

By utilizing the gauge data, $P_g(\vec{x}_i)$, radar data, $R(\vec{x}_i)$, and elevation $E(\vec{x}_i)$ the regression coefficient $\beta_{o,}$ β_1 and β_2 can be calculated by the Generalized Least Squares (GLS) method. Also, the residuals $\varepsilon(\vec{x}_i)$ need to be calculated. Through known values of regression coefficient β_0, β_1, β_2 and corresponding radar data, $R(\vec{x}_i)$, and elevation $E(\vec{x}_i)$, the regression estimates at any ungauged locations $\vec{x}_p$ can be calculated by using $\beta_o + \beta_1 R(\vec{x}_p) + \beta_2 E(\vec{x}_p)$ where $\vec{x}_p = (x_p, y_p)$ the position vector of ungauged locations. The continuous trend surface can therefore be obtained with the regression values computed at the centroid of each cell of the radar grids. Then, the deterministic part is completed with estimates regression values.

The Kriging technique is followed to find the potential residuals, $\varepsilon(\vec{x}_p)$, at any ungauged locations by summing the multiplication of Kriging weights and the corresponding residuals at ungauged locations to give

$$\varepsilon(\vec{x}_p) = \sum_{i=1}^{n} \omega_{ip} \varepsilon(\vec{x}_i), \tag{5.3}$$

where ω_{ip} is the Kriging weights at $\vec{x}_i$with respect to $\vec{x}_p$. In order to find Kriging weights semivariance analysis is used. The semivariance analysis utilizes the residuals differences between gauge pairs and the separated distance h as shown below

$$\gamma(h) = \frac{1}{2n(h)} \sum_{i=1}^{n(h)} \left(\varepsilon(\vec{x}_i) - \varepsilon\left(\overrightarrow{x_\iota + h}\right)\right)^2, \tag{5.4}$$

where *n(h)* is the number of pairs of residuals separated by h, $\varepsilon(\vec{x}_i)$ is the residuals at the location $(\vec{x}_i)$ and $\varepsilon(\overrightarrow{x_\iota + h})$ is the residuals away from $\varepsilon(\vec{x}_i)$ by a distance h.

In this study, in order to calculate the residual differences between gauge stations, elevation is also taken into account for the distance calculation and the results are compared with these using 2D distance.

Semivariogram can be constructed by plotting the data of semivariance versus distance using Equation (5.4). For the present study, the fitted function describing the constructed semivariogram follows the spherical model. Figures 5.1 and 5.2 show examples of semivariogram using respectively for 2D and 3D distance for typhoon Kalmaegi.

The function of the established semivariograms are then used to form the following equation for the determination of the Kriging weights (ω_{ip}) as

$$\begin{bmatrix} \omega_{1p} \\ \omega_{2p} \\ \omega_{3p} \\ \vdots \\ \vdots \\ \omega_{np} \\ \mu \end{bmatrix} = \begin{bmatrix} \gamma_{11} & \gamma_{12} & \cdots & \cdots & \gamma_{1n} & 1 \\ \gamma_{21} & \gamma_{22} & \cdots & \cdots & \gamma_{2n} & 1 \\ \gamma_{31} & \gamma_{32} & \cdots & \cdots & \gamma_{3n} & 1 \\ \vdots & \vdots & \cdots & \cdots & \vdots & 1 \\ \vdots & \vdots & \cdots & \cdots & \vdots & 1 \\ \gamma_{n1} & \gamma_{n2} & \cdots & \cdots & \gamma_{nn} & 1 \\ 1 & 1 & \cdots & \cdots & 1 & 1 \end{bmatrix}^{-1} \begin{bmatrix} \gamma_{1p} \\ \gamma_{2p} \\ \gamma_{3p} \\ \vdots \\ \vdots \\ \gamma_{np} \\ 1 \end{bmatrix}. \tag{5.5}$$

Here, γ_{ij} is the semivariance of paired rain gauge stations, γ_{ip} is the semivariances according to the distance between at ungauged point $\vec{x}_p$ and gauged point $\vec{x}_i$. μ is the Lagrange multiplier. Thus, the contributions of the stochastic part can be evaluated and summed with the values from the deterministic part to have the eventual adjustments of rainfall rate at any ungauged locations. We have

$$R(\vec{x}_p) = \beta_0 + \beta_1 R(\vec{x}_p) + \beta_2 E(\vec{x}_p) + \sum_{i=1}^{n} \omega_{ip} \varepsilon(\vec{x}_i). \quad (5.6)$$

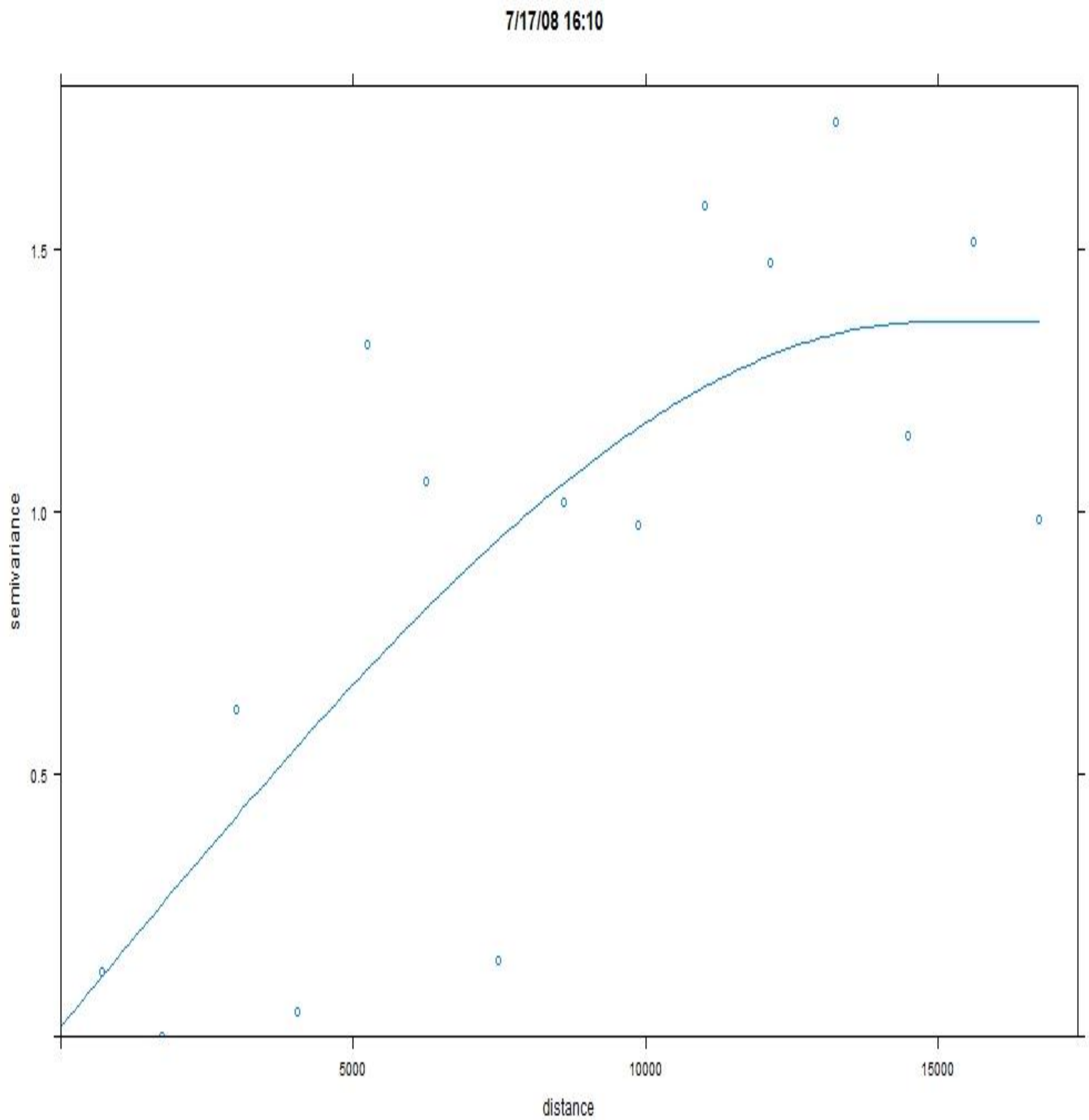

Figure 5.1. Sample 2D Semivariogram for typhoon Kalmaegi

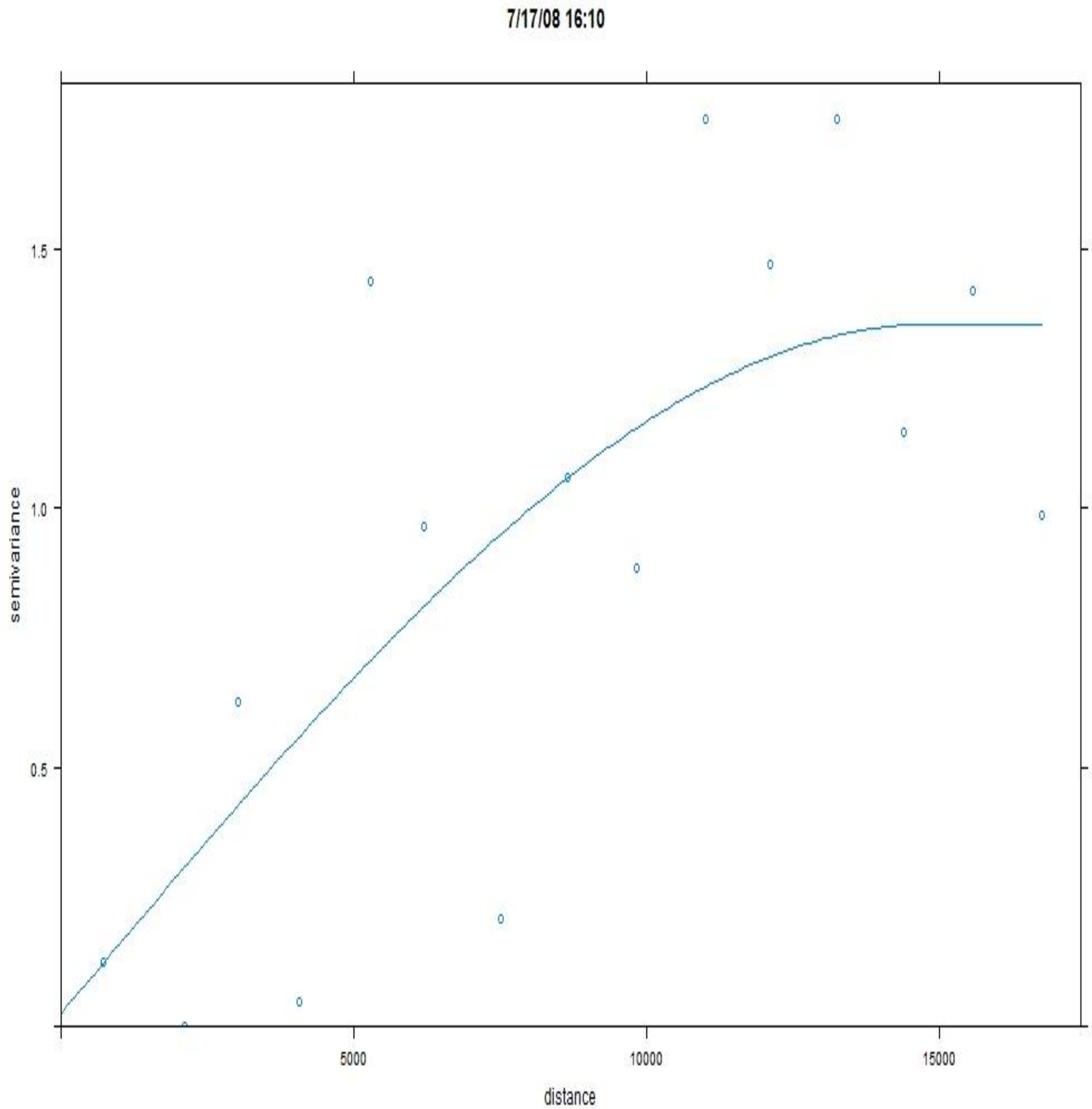

Figure 5.2. Sample 3D Semivariogram for typhoon Kalmaegi

5.2 Merging Method

The Merging method (Ehret, 2003) is also applied in this study to correct the radar rainfall data according to the rain gauge observations. The idea behind the Merging method is to combine the rain fields interpolated from rain gauge data with the spatial adjustments of radar data to obtain the final rain fields after the corrections. This procedure first estimates the rainfall rate at any ungauged locations using the Kriging approach as

$$R_{rg}(\vec{x}_p) = \sum_{i=1}^{n} \omega_{ip} R_g(\vec{x}_i), \tag{5.7}$$

where $R_{rg}(\vec{x}_p)$ is rainfall rate at an ungauged location $\vec{x}_p$, $\vec{x}_i$ is the position vector of the *i*th gauge station, $R_g(\vec{x}_i)$ is the gauge measurements at $(\vec{x}_i)$, ω_{ip} is the Kriging weights, and n is the total number of rain gauge stations. The Kriging weights can be obtained from Equation (5.5) through ordinary Kriging procedure. But in the calculation, rain gauge data R_g are used instead of residuals ε as shown in Equation (5.4). The results are applied at the centroid of each cell of the radar grids assigned on the study area.

The next step is to determine the spatial distribution adjustments at any ungauged locations by using the radar rainfall estimates and the equation given below

$$\Delta R(\vec{x}_p) = R_r(\vec{x}_p) - \sum_{i=1}^{n} \omega_{ip} R_r(\vec{x}_i), \tag{5.8}$$

where $\Delta R(\vec{x}_p)$ is the spatial rainfall adjustment at an ungauged location $\vec{x}_p$, $R_r(\vec{x}_p)$ is the unadjusted radar rainfall rate at $\vec{x}_p$, $R_r(\vec{x}_i)$ is the unadjusted radar rainfall rate at $\vec{x}_i$. Thus, the final rainfall rate can be obtained by summing the results from Equation (5.7) and (5.8) as

$$R(\vec{x}_p) = R_{rg} + \Delta R(\vec{x}_p), \tag{5.9}$$

where $R(\vec{x}_p)$ is the final rain field at $\vec{x}_p$.

6 Results

Two geostatically based spatial interpolation techniques, RK and Merging, as described in Chapter 5 are applied in the Chenyulan river watershed by using the rainfall data recorded from five typhoon event hit Taiwan. The five typhoons include typhoon Kalmaegi, typhoon Fungwong, Typhoon Sinlaku, typhoon Morakot and typhoon Fanapi. The calculations were first performed with the 2D distance based semi between rain gauges and then 3D true distance determined semi for the corrections of radar rainfall data. The results are compared to examine the effect of 3D distance on the RK and Merging methods. The Leave one out cross validation (LOOCV) techniques are selected to analyze the accuracy of the rain fields obtained from the RK, Merging and Ordinary Kriging (OK) methods. The observed rainfall data from one of the rain gauge stations are first taken out and the data from the remaining rain gauge stations are used to obtain the estimated rainfall values at the location that is left out for the interpolation procedure. The LOOCV procedure continues until all gauge stations are tested. The results from three rain gauge stations, C1M440, C1I060 and C1I080, representing respectively the positions of upstream, central region, and downstream of the watershed are selected to make the comparisons between the observed and adjusted (interpolated) rainfall values with error analysis and time series and scatter plots.

For the error analysis, Root Mean Squared Errors (RMSE) are calculated for the five typhoon events, where the RMSE has the following of

$$RMSE(x_i) = \sqrt{\frac{\sum_{t=1}^{n}\left(R_t(\vec{x}_i) - R_{gt}(\vec{x}_i)\right)^2}{n}}, \tag{6.1}$$

where $\vec{x}_i$ is the position vector of the ith rain gauge station, $R_t(x_i)$ is the adjusted rainfall value at $\vec{x}_i$, $R_{gt}(x_i)$ is the observed gauge measurements at $\vec{x}_i$, t is the time, n is the total number of selected rainfall measurements from a time series data. Smaller value of RMSE represents a better prediction.

Additionally, the time series plots are generated to compare the adjusted radar rainfall rates obtained from RK, Merging and OK methods with the unadjusted radar rainfall measurements from QPESUMS system. For this comparison study, peak hours are selected for time series plots under each typhoon event. Also, the scatter plots to present the direct and the interpolated radar rainfall rates provided by RK, Merging, and OK or the unadjusted radar rainfall values at selected rain gauge stations are constructed. In order to show if the results having better estimate values, the reference 45 degree lines are also included in the plots. The points which are closer to the reference 45 degree line indicate the better predictions obtained.

6.1 Typhoon Kalmaegi

The RMSE of the adjusted rainfall rates obtained from RK, Merging and OK according to the inputs of 2D and 3D distances are computed by comparing to the true measurements from rain gauge stations. As a reference, the RMSE of the unadjusted QPESUMS data are also calculated. A summary of the above described RMSE values for each station is given in Table 6.1. The percentages of improvement for the adjusted values are evaluated by comparing with the QPESUMS`s results. A positive improving percentage represents a better approach for adjusting radar rainfall data while a negative percentage denotes the less accurate adjustment procedure. Also, the RMSEs and percentages of improvements obtained from using the 2D distance and 3D distance approaches are also compared to evaluate the effect of distance on the adjusted values. Figures 6.1(a), 6.1(b), and 6.1(c) show the percentages of the improvement of 2D and 3D distance results by RK, Merging and OK, respectively. Comparing the percentages of improvement from 2D and 3D distance approaches, the differences of those values are calculated from RK, Merging and OK methods and the results are plotted in Figure 6.2. A positive difference indicates using 2D distances gives better estimates whereas a negative differences suggests the use of 3D distances produces more accurate estimates than those using 2D distances.

Among the selected reference stations the estimations obtained from RK, Merging, and OK at the station C1M440 are to have slightly different RMSEs with values of 0.9519 mm (RK), 0.9096 mm (Merging), and 0.9830 mm (OK) from using 3D distance based approaches and 0.8672 mm (RK), 0.7664 mm (Merging), and 0.8512 mm (OK) from 2D distance based calculations. The errors from 2D distance approaches appear to be slightly less than those from 3D distance based methods for stations C1M440. For the other two reference stations (C1I300 and C1I060) it is found the adjusted rainfall values (or errors) are similar for the methods used with the inputs of either 2D or 3D distances.

By examining the results of percentage of improvement presented in the Table 6.1 and Figures 6.1(a) – 6.1(c), we notice that the Merging method gives overall better estimates of radar rainfall values than RK and OK methods do for the scenarios of using either 2D or 3D distance in the calculation of all stations. When considering the overall average of the improving percentages, the estimated rainfall rates using the inputted 2D distances seem to be shown slightly better prediction than those using 3D distance based calculation.

Comparing station by station the 3D distance based approach reveal more improved results in 15 stations for RK, 13 stations for Merging, and 16 stations for OK method out of total 27 stations, especially for the stations located at high elevation.

Among the selected three reference stations C1M440, C1I060 and C1I300, the results using 3D distance at station C1I300 are shown to have better estimates than those with the use of 2D distances for all interpolation methods RK, Merging and OK. Apart from the reference stations the estimates at stations C1I310, C0I090, C1I290, C1I070, C1V460, 467550, C1I040, 1510P030 and 1730P132 are also shown to give better predictions when 3D distances between rain gauges are used in the corresponding calculations.

Table 6.1.RMSE analysis based on RK, Merge and OK by using 2D and 3D distance for Typhoon Kalmaegi

STATION ID	Elevation (m)	QPESUMS (mm)	RK					MERGING					OK				
			2D		3D		2D -3D	2D		3D		2D -3D	2D		3D		2D -3D
			(mm)	impr %	(mm)	impr %		(mm)	impr %	(mm)	impr %		(mm)	impr %	(mm)	impr %	
C1I270	593	0.9356	0.7880	15.7739	0.8473	9.4418	6.3321	0.7805	16.5814	0.8717	6.8350	9.7463	1.1668	-24.7109	1.1636	-24.3669	-0.3440
C1I150	393	1.1093	1.0552	4.8780	1.0610	4.3577	0.5203	1.0052	9.3848	0.9942	10.3815	-0.9966	1.1161	-0.6076	1.1033	0.5402	-1.1477
C1I160	399	1.1745	0.8457	27.9948	0.8613	26.6680	1.3268	0.8485	27.7542	0.8560	27.1152	0.6390	0.8572	27.0130	0.8823	24.8803	2.1328
C1I310	1001	1.1615	0.8093	30.3185	0.7744	33.3313	-3.0129	0.8271	28.7903	0.7715	33.5784	-4.7881	0.8657	25.4656	0.8142	29.9033	-4.4378
C1I300	781	1.0986	0.8842	19.5124	0.8821	19.7051	-0.1927	0.8220	25.1783	0.7829	28.7392	-3.5610	0.8987	18.1980	0.8500	22.6302	-4.4322
C0I090	878	1.2969	1.2340	4.8439	1.1991	7.5381	-2.6942	1.2107	6.6425	1.1835	8.7402	-2.0977	1.5587	-20.1906	1.5181	-17.0642	-3.1264
C1I100	1771	NA	NA	NA	NA	NA	NA	NA	NA	NA	NA	NA	NA	NA	NA	NA	NA
C1I120	1528	1.3382	1.6449	-22.9168	1.6548	-23.6514	0.7346	1.2607	5.7945	1.2514	6.4894	-0.6949	1.5634	-16.8287	1.5546	-16.1695	-0.6592
C1I290	1151	1.2723	1.4387	-13.0765	1.3885	-9.1279	-3.9486	0.9591	24.6204	0.9514	25.2241	-0.6038	1.0527	17.2603	1.0504	17.4440	-0.1837
C1I080	536	1.3154	1.0628	19.2024	1.0642	19.0991	0.1033	0.9274	29.4947	0.8972	31.7930	-2.2982	1.0925	16.9416	1.0519	20.0310	-3.0893
C1I060	1181	1.2888	1.1406	11.5039	1.1056	14.2148	-2.7109	0.7144	44.5720	0.7216	44.0125	0.5595	0.8575	33.4656	0.8708	32.4346	1.0311
C1I070	825	1.1138	0.8599	22.7965	0.8266	25.7824	-2.9859	0.8701	21.8804	0.8048	27.7466	-5.8662	0.8981	19.3648	0.8535	23.3697	-4.0048
C1I340	897	1.1850	0.9855	16.8330	0.9719	17.9825	-1.1496	0.9296	21.5548	0.9301	21.5072	0.0476	0.9351	21.0855	0.9349	21.1027	-0.0172
C1I350	887	1.1167	0.8968	19.6914	0.9423	15.6205	4.0708	0.9434	15.5147	0.9853	11.7662	3.7485	0.9398	15.8413	0.9812	12.1379	3.7034
C0H9A0	1595	1.1829	1.1218	5.1720	1.0941	7.5068	-2.3348	0.9776	17.3554	0.9818	17.0064	0.3490	0.9818	17.0073	0.9743	17.6378	-0.6306
C1V460	1949	1.1922	1.1127	6.6713	1.1047	7.3421	-0.6708	1.0802	9.3951	1.0644	10.7254	-1.3303	1.1677	2.0593	1.1363	4.6903	-2.6310
C1M440	2540	1.1680	0.8672	25.7564	0.9519	18.5029	7.2535	0.7664	34.3848	0.9096	22.1264	12.2583	0.8512	27.1288	0.9830	15.8432	11.2855
C1V170	3690	0.8517	0.6974	18.1119	0.7516	11.7481	6.3637	0.7240	14.9947	0.7586	10.9247	4.0699	0.9206	-8.0910	0.9453	-10.9935	2.9025
C1M630	1052	1.2867	2.0776	-61.4711	2.0678	-60.7102	-0.7609	1.2367	3.8792	1.2941	-0.5822	4.4614	2.1376	-66.1343	2.1561	-67.5748	1.4405
X467550	3845	1.1010	1.0780	2.0895	1.0677	3.0179	-0.9284	1.0564	4.0447	1.0502	4.6089	-0.5641	1.0947	0.5663	1.0904	0.9568	-0.3905
X467530	2413	1.6368	1.4538	11.1817	1.4733	9.9908	1.1909	1.5225	6.9824	1.5725	3.9265	3.0559	1.5435	5.7001	1.5876	3.0069	2.6932
C1I170	235	1.1718	1.2174	-3.8878	1.2344	-5.3371	1.4493	1.2092	-3.1886	1.2249	-4.5300	1.3414	1.7710	-51.1290	1.8022	-53.7959	2.6669
C1I040	1693	1.1601	1.1917	-2.7193	1.1883	-2.4268	-0.2925	1.1951	-3.0110	1.1752	-1.3010	-1.7100	1.4049	-21.0955	1.3736	-18.3989	-2.6965
X1510P088	1666	1.2629	1.0049	20.4302	1.0103	20.0047	0.4255	1.0486	16.9688	1.0583	16.2016	0.7672	1.0554	16.4334	1.0706	15.2305	1.2029
X1510P087	2200	1.1384	0.7927	30.3684	0.7555	33.6320	-3.2636	0.5618	50.6442	0.5892	48.2394	2.4049	0.5489	51.7859	0.5655	50.3206	1.4653
X1510P030	1135	1.6099	1.5852	1.5379	1.5662	2.7156	-1.1777	1.5578	3.2368	1.5354	4.6306	-1.3938	1.5887	1.3168	1.5682	2.5928	-1.2760
X1730P132	2540	1.5925	1.3309	16.4270	1.2940	18.7447	-2.3177	1.2967	18.5766	1.2884	19.1011	-0.5244	1.2598	20.8933	1.2518	21.3989	-0.5056
AVERAGE		1.1985	1.1604		1.1609			1.0003		1.0091			1.1870		1.1901		

`

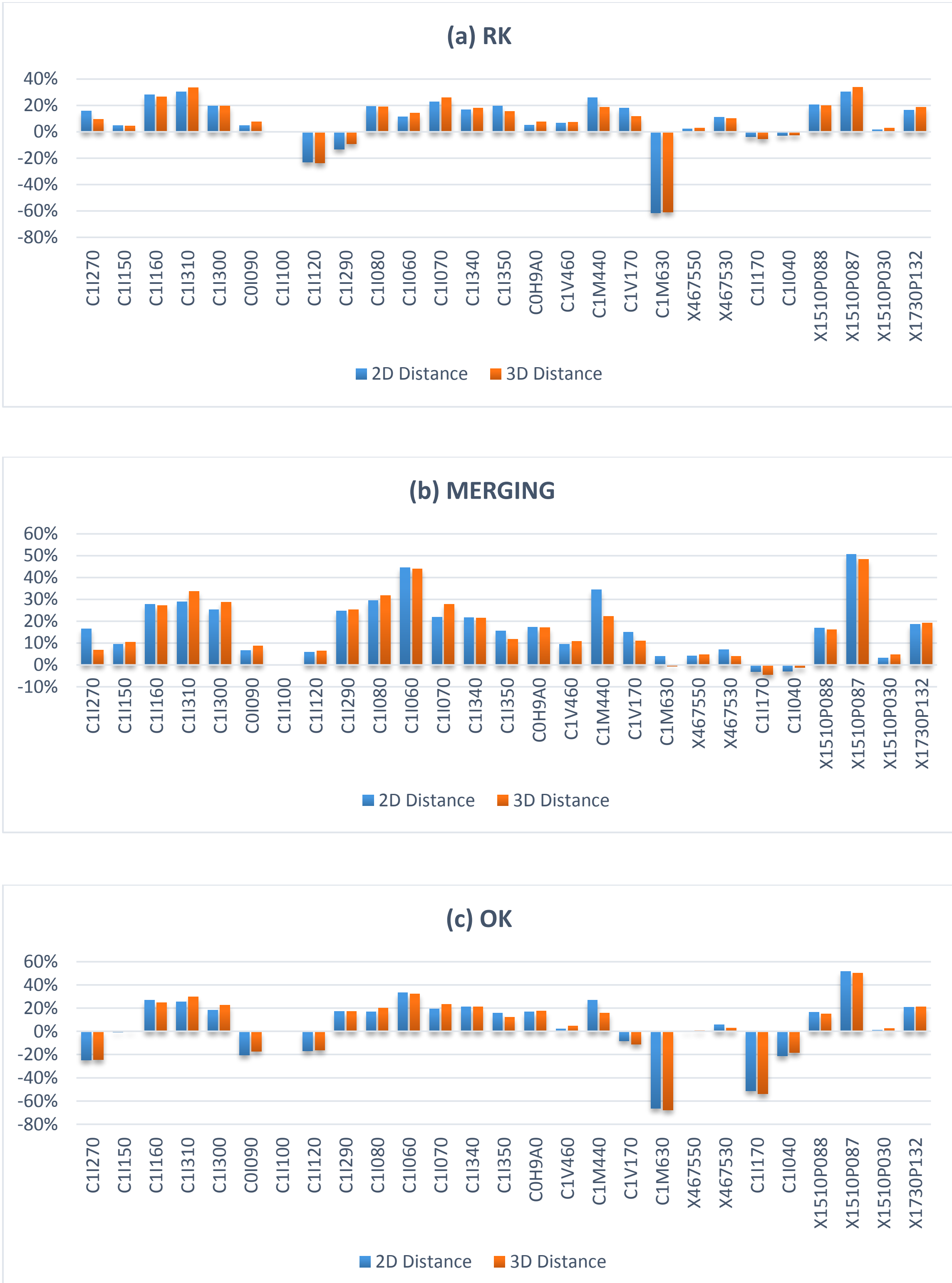

Figure 6.1. Improvements by RK, Merging and OK method with 2D and 3D distance for Typhoon Kalmaegi

`

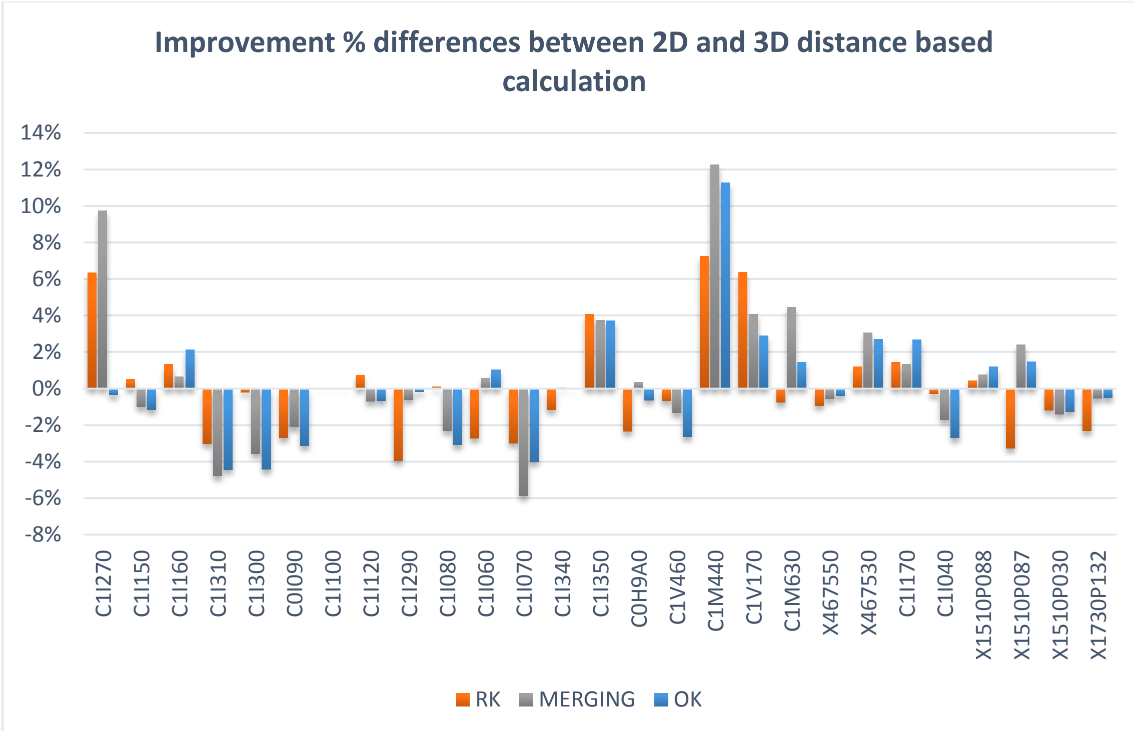

Figure 6.2. Improvement differences between 2D and 3D rain gauge distance for Typhoon Kalmaegi

For the convenience of comparing results obtained from the methodologies used, time series plots of rainfall values near the peak hour are shown in Figures 6.3(a) – 6.3(c) and Figures 6.4(a) – 6.4(c) for the use of 2D distance and 3D distance, respectively, for the selected stations. The gauge data and QPESUMS original rainfall estimates are also included in Figures 6.3(a) – 6.3(c) and Figures 6.4(a) – 6.4(c). It is noticed that the QPESUMS data as shown with a smooth curve describe only the gradual rainfall variation, while the adjusted values from RK, Merging and OK give more truly reflected fluctuations to follow closely to rain gauge values for both 2D and 3D results see in Figures 6.3(a) – 6.3(c) and Figures 6.4(a) – 6.4(c).

`

The results after the geostatistic corrections using 3D distances are shown to be similar to those obtained from 2D distance approach at the station C1I060, however to have better predictions than the 2D distance produced values at the station C1I300.

The results of adjusted rainfall rates obtained from spatial interpolation methods, RK, Merging and OK and unadjusted rainfall rate provided by QPESUMS system are plotted versus raw gauge data for direct comparisons. The results using the inputs of 2D distance are shown in Figures 6.5(a) – 6.5(c) for the three selected stations whereas the comparison results under the 3D distance cases are given in Figures 6.6(a) – 6.6(c). It is noticeable that the improved rainfall data obtained from RK, Merging, and OK by using 2D or 3D distances between rain gauges for the calculation are shown to have a narrower bandwidth to the 45 degree reference line, which suggest better estimated radar rainfall rates while the values of QPESUMS are scattered with wider bandwidth to the reference line indicating less accurate estimates.

`

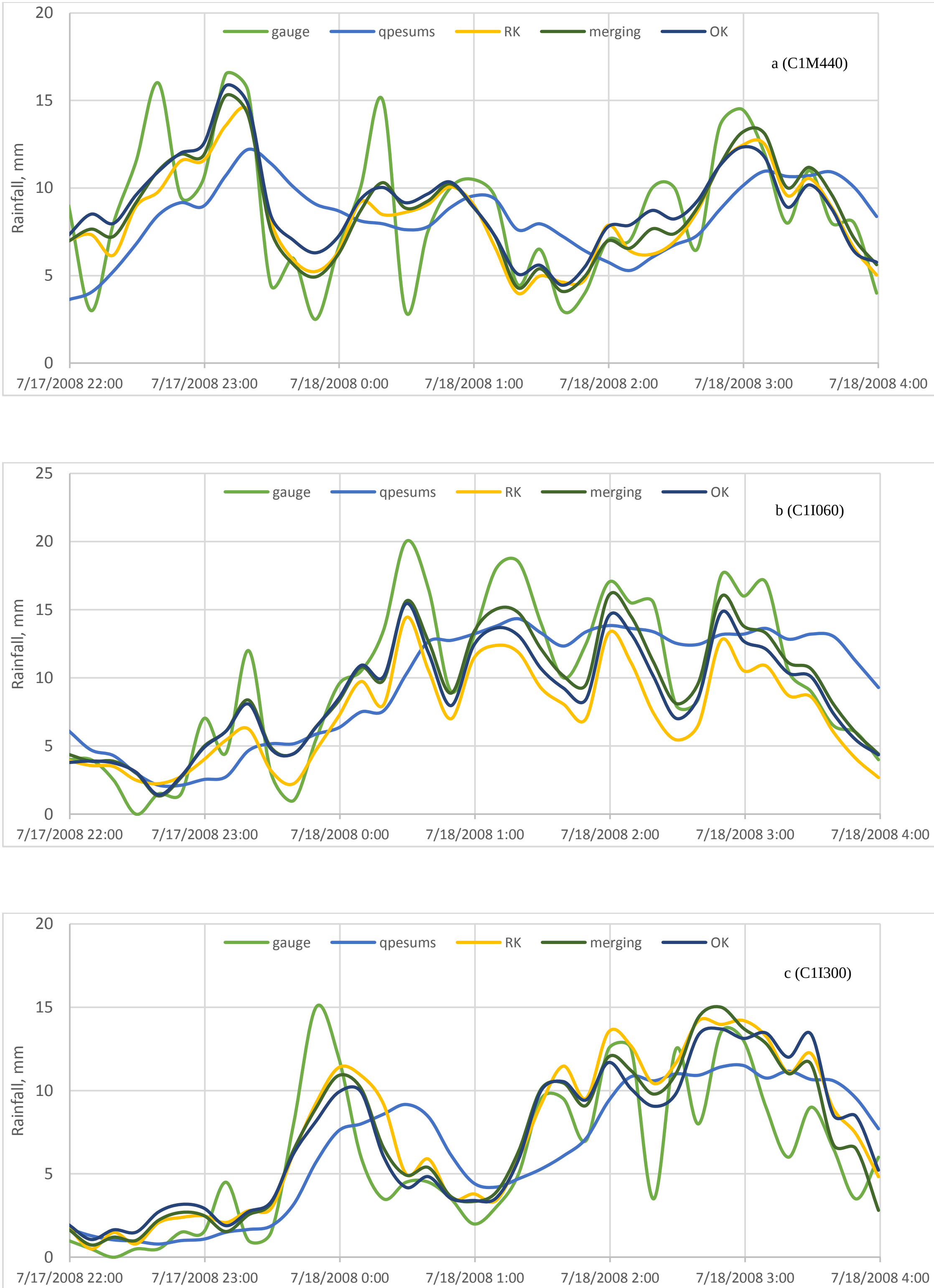

Figure 6.3. Peak hour comparison by using 2D distance for Typhoon Kalmaegi

`

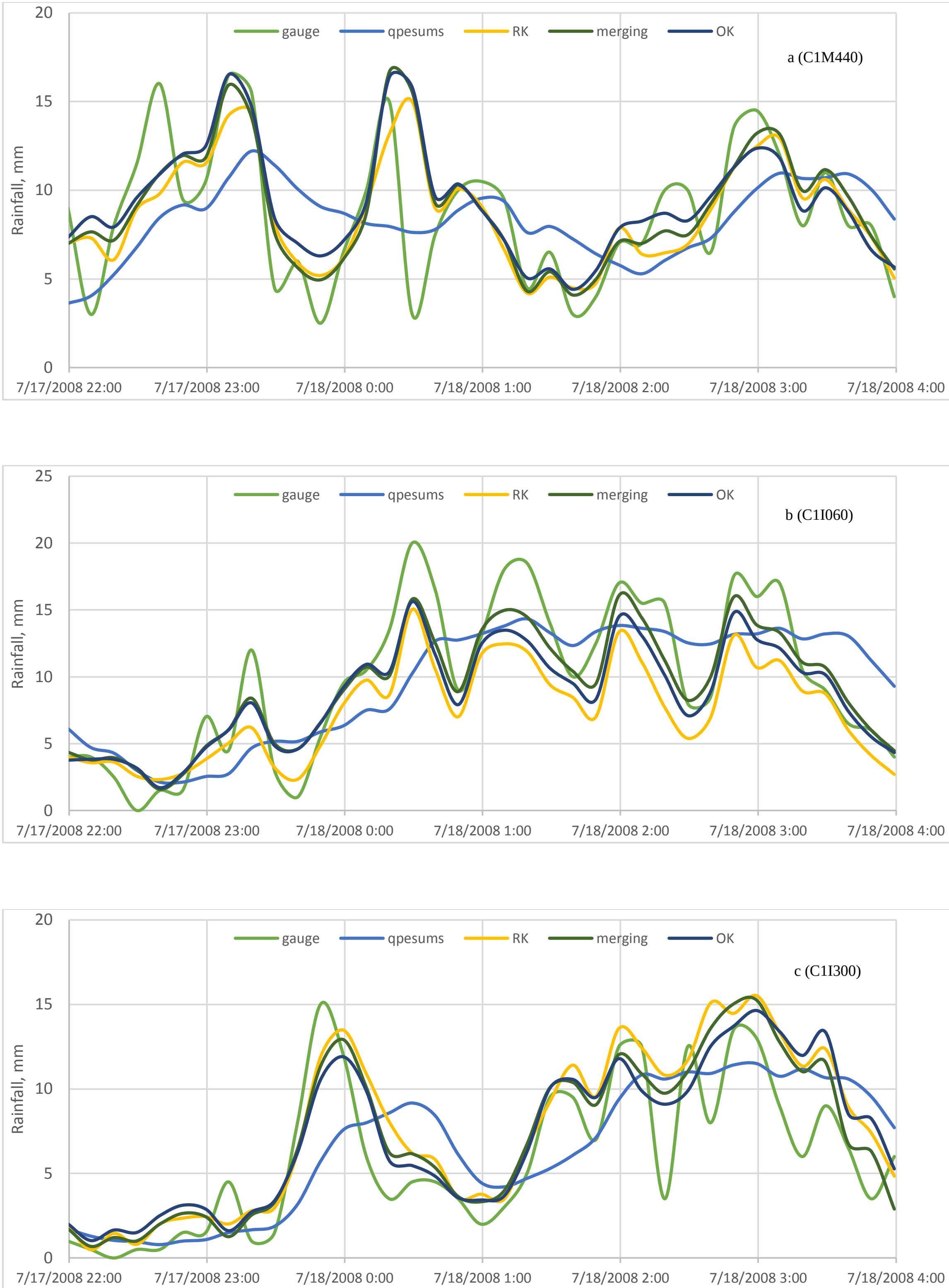

Figure 6.4. Peak hour comparison by using 3D distance for Typhoon Kalmaegi

`

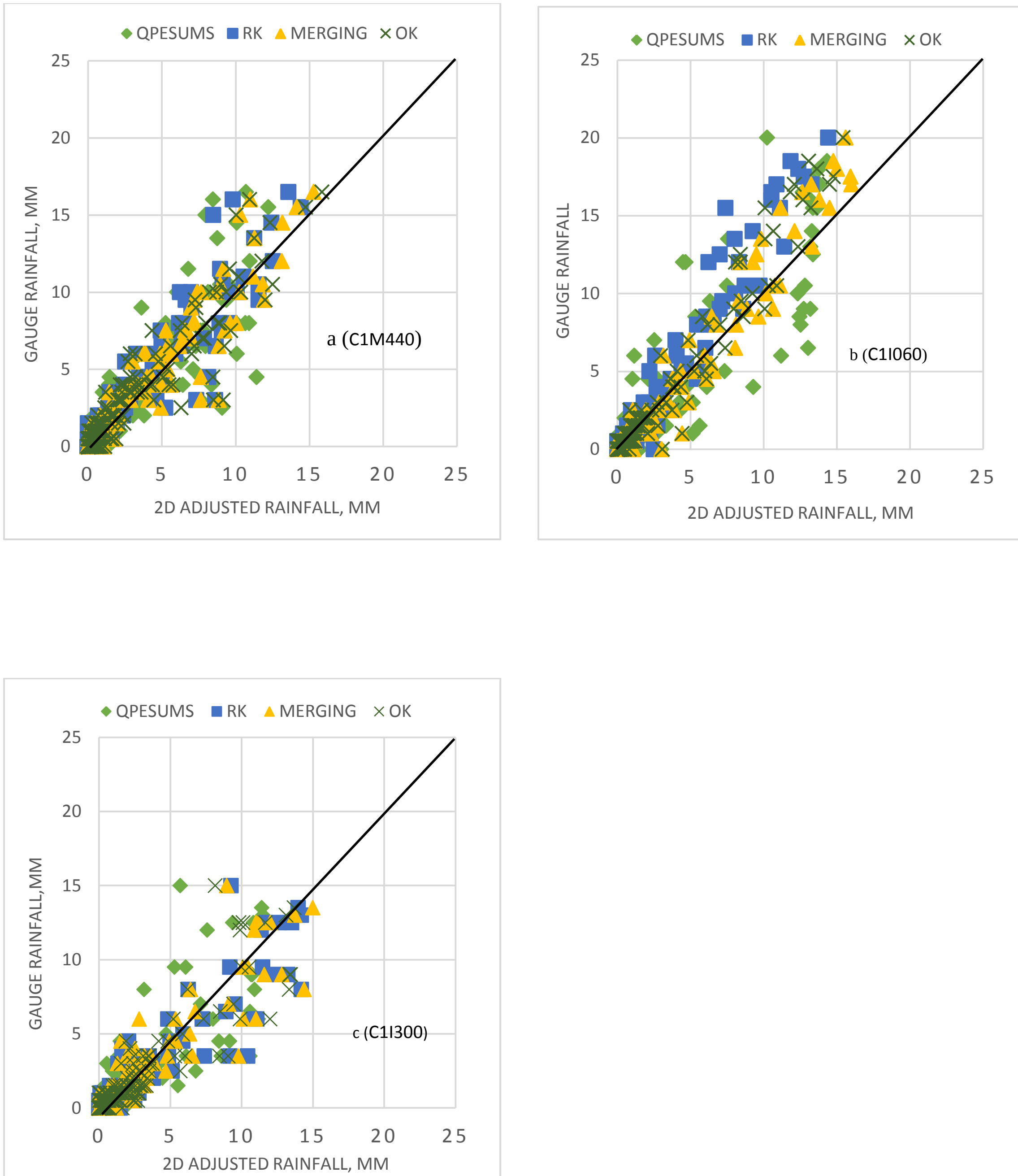

Figure 6.5. Adjusted Rainfall Rate using 2D distance versus Unadjusted Rainfall Rate obtained from Rain Gauges for typhoon Kalmaegi

`

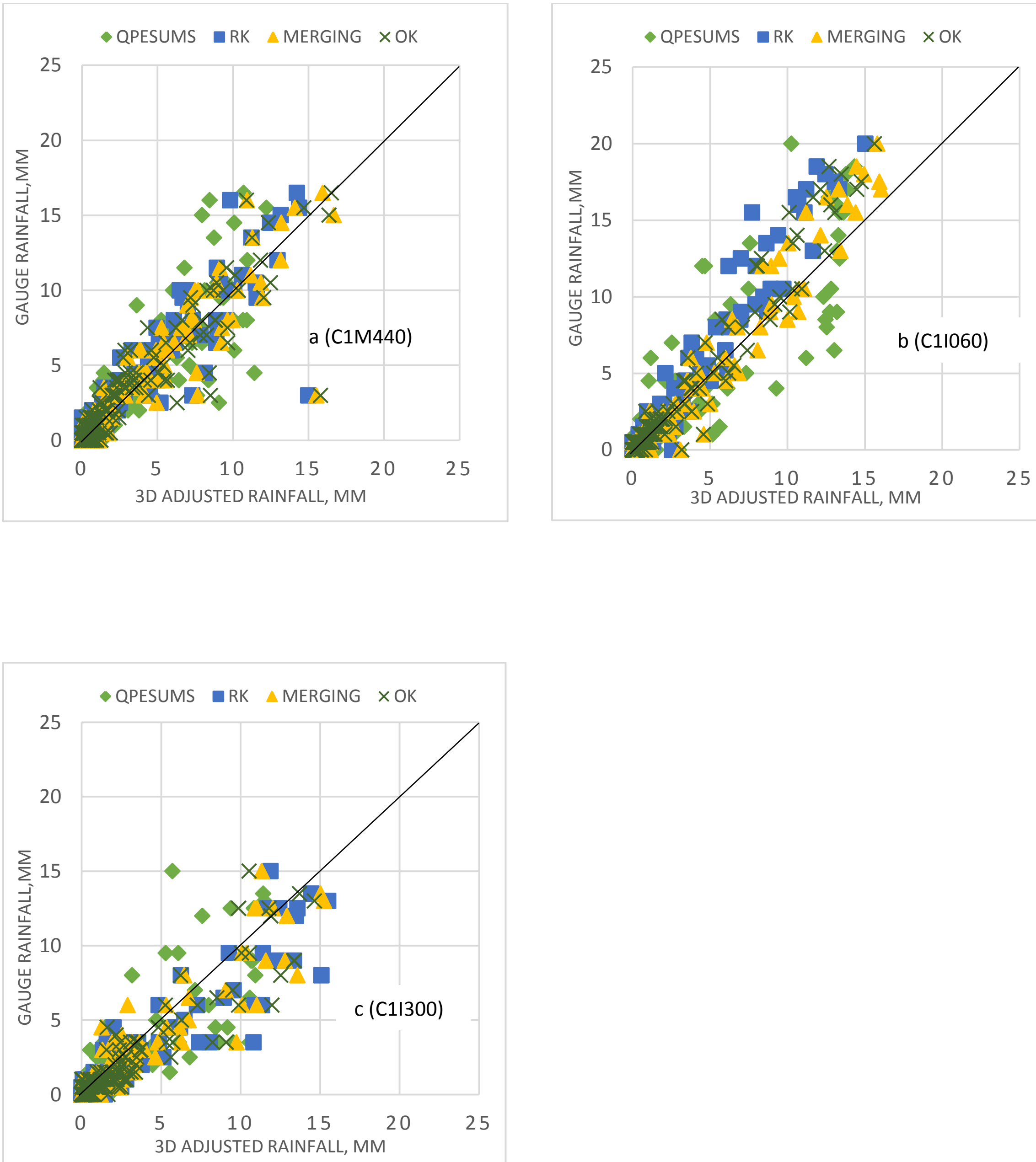

Figure 6.6. Adjusted Rainfall Rate using 3D distance versus Unadjusted Rainfall Rate obtained from Rain Gauges for typhoon Kalmaegi

`

6.2 Typhoon Morakot

The correction of radar rainfall rates by RK, Merging and OK methods are also performed for the event of typhoon Morakot. The errors based on the RMSE, percentage of improvement, time series plots and the scatter plots of direct comparisons of showing the level of agreement as reflected along the 45 degree reference line between the rain gauge data and the adjusted and unadjusted rainfall rates are analyzed. The adjusted results include these using inputs of 2D distances or 3D distances. Table 6.2 summaries the results of RMSE for the rainfall values from RK, Merging and OK and those unadjusted QPESUMS data. The results in Table 6.2 indicate that the Merging method produces the best predictions using either 2D or 3D distances comparing to the RK and OK approaches. Again using 2D distances between rain gauges in the calculation produces slightly better estimates than using 3D distances. The average RMSEs for RK, Merging and OK methods by using 2D distances are respectively 1.0353 mm, 0.9442 m and 1.1316 mm. Those values becomes 1.0479 mm (RK), 0.9538 mm (Merging), and 1.1399 mm (OK) when 3D distances are used.

In addition to the error analysis, the percentages of improvement for the results using either 2D or 3D rain gauge distances are presented in Figures 6.7(a), 6.7(b), and 6.7(c) for RK, Merging, and OK methods respectively. The differences of percentage using improvement between 2D and 3D distance result for RK, Merging and OK methods are shown in Figure 6.8. It can be seen from Figure 6.7 that Merging method gives overall better estimates than does RK or OK for the improvement of QPESUMS data. It is noted that missing rainfall measurements at station C1I120 were observed and error anlysis exluded from that station.

Table 6.2. RMSE analysis based on RK, Merge and OK by using 2D and 3D distance for Typhoon Morakot

STATION ID	Elevation (m)	QPESUMS (mm)	RK					MERGING					OK				
			2D		3D		2D -3D	2D		3D		2D -3D	2D		3D		2D -3D
			(mm)	impr %	(mm)	impr %		(mm)	impr %	(mm)	impr %		(mm)	impr %	(mm)	impr %	
C1I270	593	0.8098	0.5320	34.3118	0.5333	34.1447	0.1671	0.6513	19.5760	0.6599	18.5060	1.0700	0.8399	-3.7145	0.8466	-4.5398	0.8253
C1I150	393	0.9292	0.6704	27.8461	0.6923	25.4930	2.3531	0.7186	22.6581	0.7409	20.2594	2.3987	0.9546	-2.7392	0.9709	-4.4965	1.7572
C1I160	399	0.9432	0.4944	47.5773	0.4962	47.3944	0.1829	0.5382	42.9393	0.5377	42.9892	-0.0498	0.5806	38.4449	0.5833	38.1535	0.2914
C1I310	1001	0.9201	0.4693	48.9986	0.4710	48.8124	0.1862	0.4589	50.1271	0.4589	50.1257	0.0015	0.5012	45.5319	0.5014	45.5060	0.0260
C1I300	781	0.7982	0.5688	28.7314	0.5755	27.8918	0.8396	0.5808	27.2332	0.5803	27.2971	-0.0639	0.6933	13.1422	0.7005	12.2335	0.9087
C0I090	878	1.2537	1.0939	12.7453	1.1338	9.5649	3.1804	1.0292	17.9071	1.0208	18.5790	-0.6720	1.4986	-19.5310	1.5185	-21.1173	1.5864
C1I100	1771	0.7361	0.9379	-27.4106	0.9642	-30.9739	3.5633	0.7489	-1.7293	0.7581	-2.9775	1.2482	1.1219	-52.3972	1.1422	-55.1635	2.7663
C1I120	1528	NA	NA	NA	NA	NA	NA	NA	NA	NA	NA	NA	NA	NA	NA	NA	NA
C1I290	1151	1.1930	1.0691	10.3890	1.0598	11.1708	-0.7817	0.7668	35.7229	0.7562	36.6142	-0.8913	0.8364	29.8939	0.8286	30.5480	-0.6540
C1I080	536	0.9870	0.6601	33.1221	0.6735	31.7626	1.3595	0.5891	40.3165	0.6010	39.1099	1.2066	0.6713	31.9833	0.6745	31.6613	0.3221
C1I060	1181	1.2233	0.8242	32.6297	0.8629	29.4608	3.1689	0.5617	54.0838	0.5851	52.1739	1.9099	0.6985	42.9032	0.7433	39.2387	3.6645
C1I070	825	1.2872	0.8025	37.6554	0.8058	37.4031	0.2523	0.8626	32.9881	0.8711	32.3288	0.6593	0.8209	36.2245	0.8260	35.8314	0.3931
C1I340	897	1.5942	1.0400	34.7592	1.0428	34.5868	0.1723	0.9358	41.2976	0.9299	41.6684	-0.3708	0.9864	38.1223	0.9828	38.3497	-0.2274
C1I350	887	1.1588	0.6494	43.9562	0.6456	44.2854	-0.3293	0.6268	45.9120	0.6242	46.1312	-0.2192	0.6432	44.4915	0.6397	44.7956	-0.3042
C0H9A0	1595	1.5937	1.3840	13.1602	1.3331	16.3514	-3.1912	1.0891	31.6630	1.0025	37.0968	-5.4338	1.1717	26.4811	1.0858	31.8722	-5.3911
C1V460	1949	1.8054	1.4435	20.0443	1.4363	20.4413	-0.3970	1.6215	10.1839	1.6124	10.6882	-0.5043	1.7127	5.1318	1.7067	5.4654	-0.3335
C1M440	2540	1.6117	1.2226	24.1407	1.2270	23.8675	0.2732	1.1778	26.9203	1.1813	26.7043	0.2160	1.2945	19.6795	1.2952	19.6341	0.0454
C1V170	3690	1.4750	1.3577	7.9485	1.3906	5.7188	2.2297	1.3442	8.8676	1.3721	6.9703	1.8973	1.7425	-18.1381	1.7673	-19.8196	1.6815
C1M630	1052	1.6002	2.3564	-47.2600	2.3770	-48.5464	1.2864	1.5309	4.3308	1.6314	-1.9495	6.2803	2.1169	-32.2937	2.1333	-33.3185	1.0248
X467550	3845	1.4249	1.3311	6.5874	1.3346	6.3385	0.2489	1.3588	4.6434	1.3667	4.0861	0.5573	1.7204	-20.7356	1.7213	-20.7948	0.0592
X467530	2413	2.1139	1.9242	8.9721	2.0014	5.3217	3.6504	1.9161	9.3564	1.9838	6.1529	3.2035	2.3364	-10.5271	2.4047	-13.7584	3.2313
C1I170	235	0.8239	0.7413	10.0261	0.7512	8.8222	1.2039	0.8416	-2.1546	0.8607	-4.4760	2.3214	1.1197	-35.9061	1.1308	-37.2589	1.3528
C1I040	1693	1.1736	0.8549	27.1592	0.8557	27.0944	0.0648	0.9028	23.0779	0.9140	22.1256	0.9523	1.2836	-9.3650	1.2800	-9.0611	-0.3039
X1510P088	1666	1.2459	0.9970	19.9729	0.9876	20.7309	-0.7580	0.9749	21.7527	0.9701	22.1337	-0.3809	0.8969	28.0083	0.8875	28.7652	-0.7569
X1510P087	2200	1.2340	0.6634	46.2409	0.6859	44.4142	1.8268	0.6060	50.8888	0.6181	49.9108	0.9780	0.6385	48.2560	0.6685	45.8244	2.4316
X1510P030	1135	1.2367	0.8496	31.3012	0.8539	30.9554	0.3457	0.7438	39.8578	0.7463	39.6534	0.2044	0.7312	40.8714	0.7326	40.7567	0.1146
X1730P132	2540	1.7662	1.4818	16.1041	1.5317	13.2807	2.8233	1.5479	12.3600	1.5855	10.2337	2.1263	1.5678	11.2354	1.6028	9.2536	1.9818
AVERAGE		1.2669	1.0161		1.0278			0.9509		0.9603			1.1223		1.1298		

`

At the stations of C1I290, C1I350, C0H9A0, C1V460 and 1510P088 using 3D distances between rain gauges produces better estimates than using 2D distance as shown in Figure 6.8. Especially the station C0H9A0 shown the best estimates when using 3D distance in the interpolation methods RK, Merging, and OK with the -3.1912, -5.4338 and -5.3911 improvement percentage respectively.

To show the performance of RK, Merging, and OK approaches and compare the adjusted rainfall rates from using 2D or 3D distances, in Figures 6.9(a) – 6.9(c) and 6.10(a) – 6.10(c) time series plots of rainfall results near the peak hour are shown under the event of Typhoon Morakot. Figures 6.9(a) – 6.9(c) are for the results using 2D distance based semivariogram whereas Figures 6.10(a) – 6.10(c) reveal the results based on the inputs of 3D distances. The estimates of adjusted rainfall obtained from RK, Merging, and OK mostly follow closely with rain gauge data as indicated in Figure 6.9(a) – 6.9(c) and 6.10(a) – 6.10(c). Differently, again the QPESUMS data miss the representation of the true rainfall values. It is noticed that the QPESUMS curve is shown to have a sharp fall at the time frame between 8/8/09 00:00 and 8/9/09 1:00, reflecting the missing data which are plotted with zero value. The missing values are added (or corrected) into the data system through the RK, Merging or OK approaches. Overall, the adjusted rainfall values using 3D distances are similar to those with inputs of 2D distances. Among the three reference stations, the results at C1I300 are again shown to have better estimated values than those at C1I060 and C1M440.

`

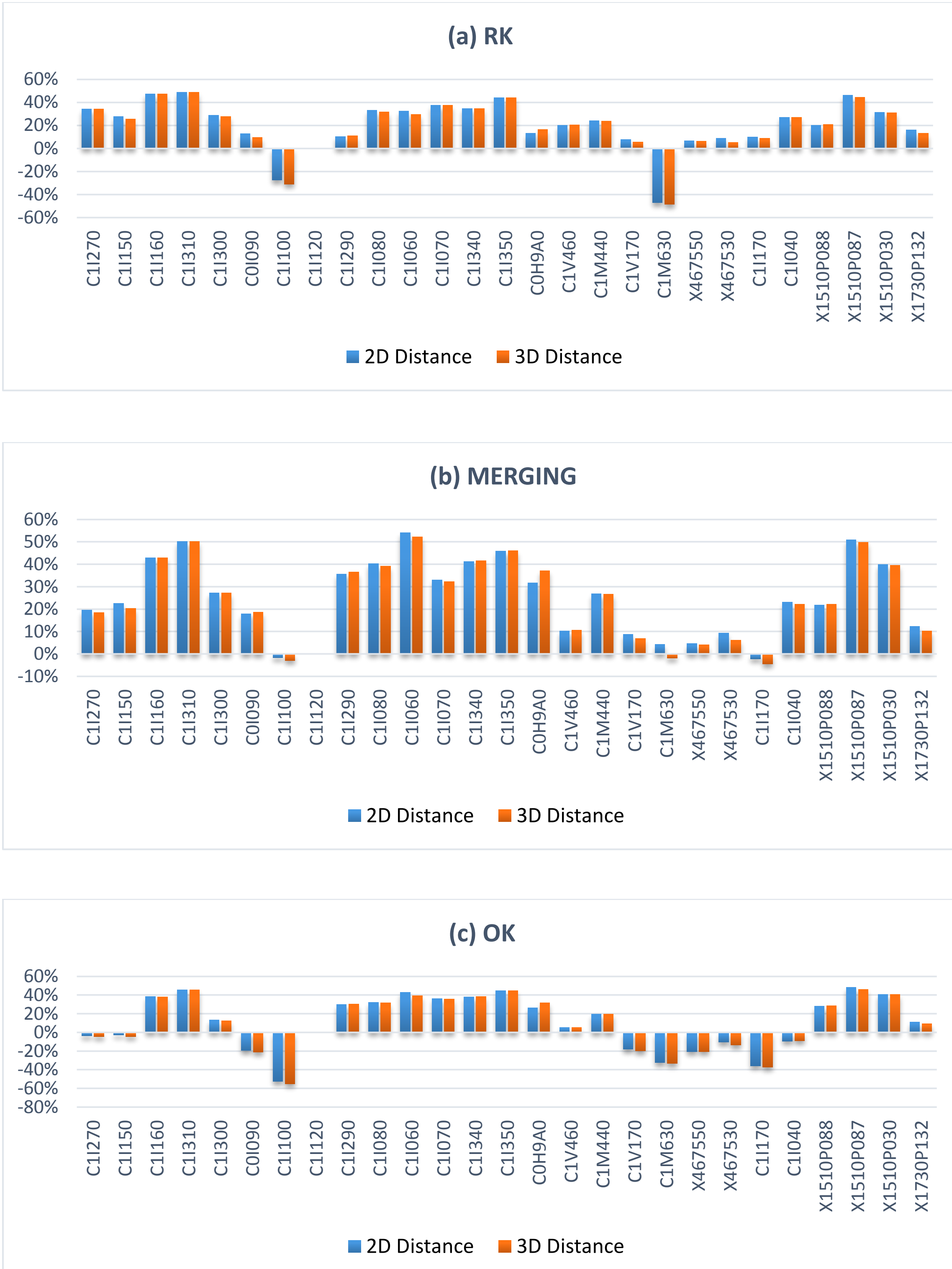

Figure 6.7. Improvements by RK, Merging and OK by 2D and 3D distance for Typhoon Morakot.

`

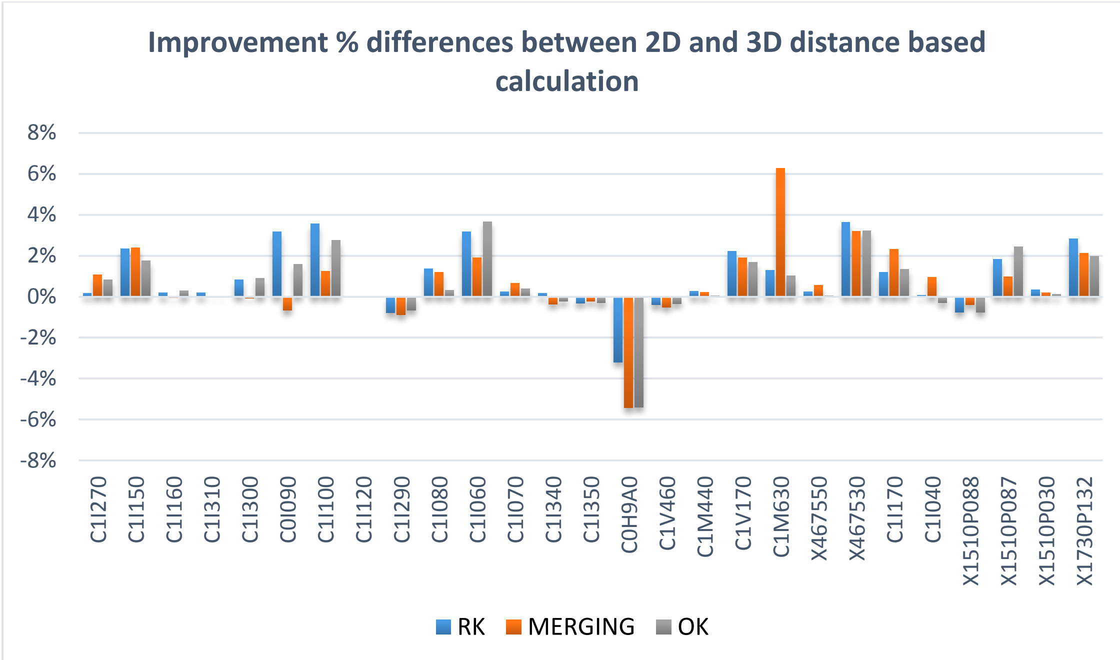

Figure 6.8. Improvement differences between 2D and 3D rain gauge distance for Typhoon Morakot.

The comparison plots between adjusted radar rainfall values and gauge data at selected reference stations for typhoon Morakot are presented in Figures 6.11(a) – 6.11(c) based on 2D distance approach and in Figures 6.12(a) - 6.12(c) using the inputs of 3D distances. It can be seen clearly again from Figures 6.11(a) – 6.11(c) and 6.12(a) - 6.12(c) that the results from QPESUMS depart from the reference 45 degree line. However, the adjusted rainfall data obtained from RK, Merging, and OK either using 2D or 3D distances are closer to the reference line indicating the improvement made to the QPESUMS estimates. Among the selected reference stations, by reviewing the results obtained rainfall from RK, Merging, and OK, we notice there is no significant advantage of using 3D distances in the calculation comparing to the traditional approach of using 2D distances as the adjusted rainfall values based on either 2D distances or 3D distances are very similar.

`

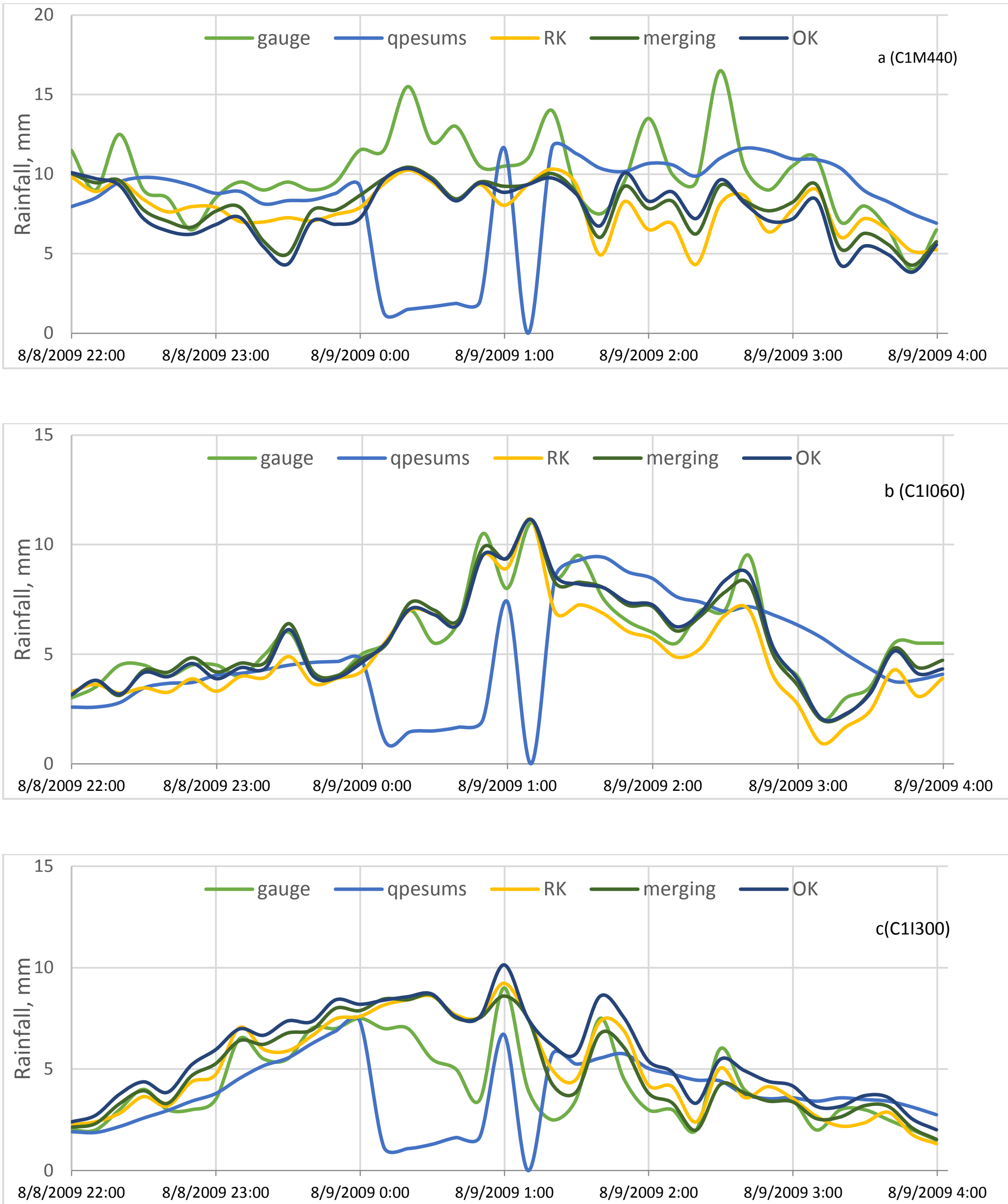

Figure 6.9. Peak hour comparison by using 2D distance for Typhoon Morakot

`

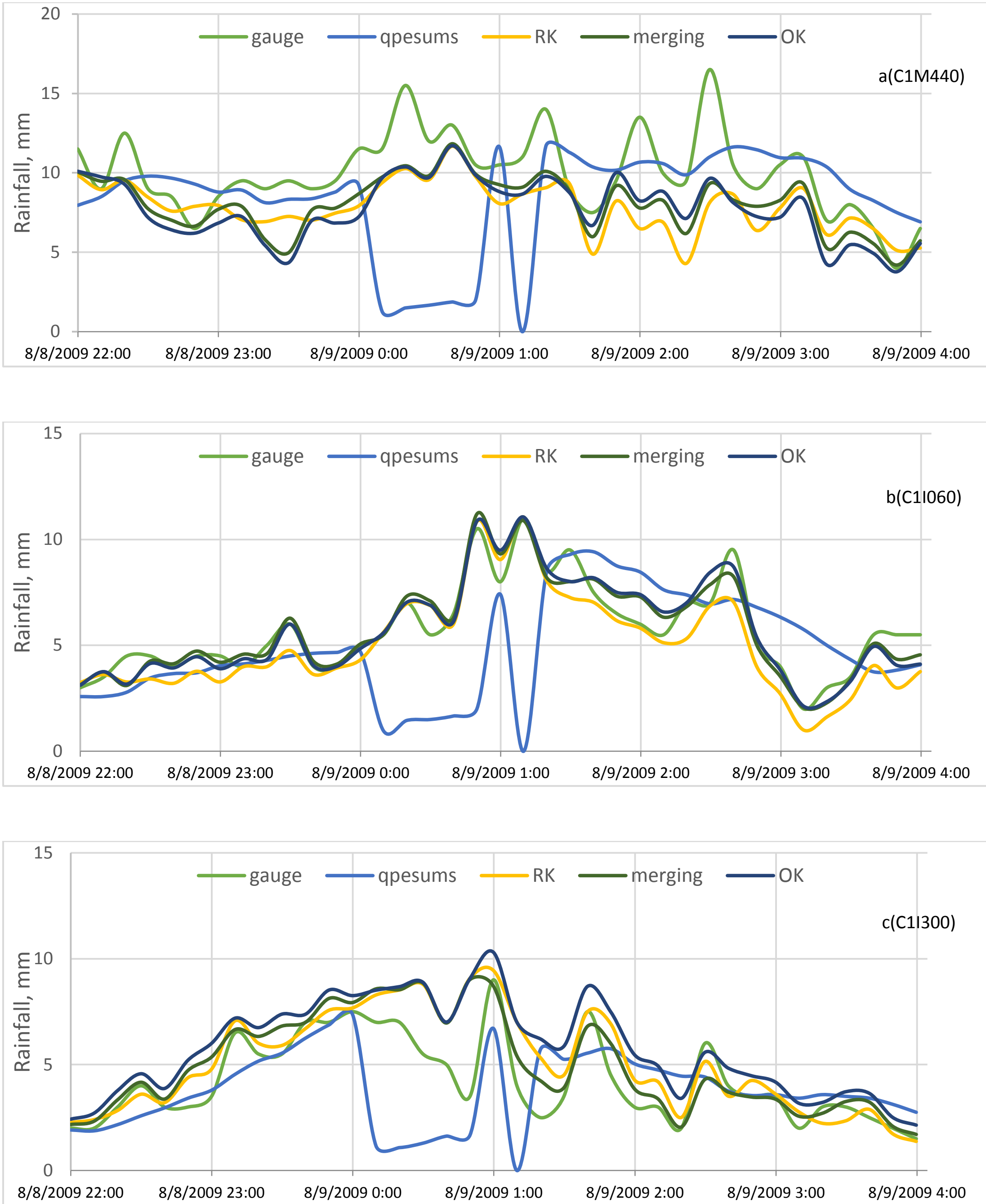

Figure 6.10. Peak hour comparison by using 3D distance for Typhoon Morakot

`

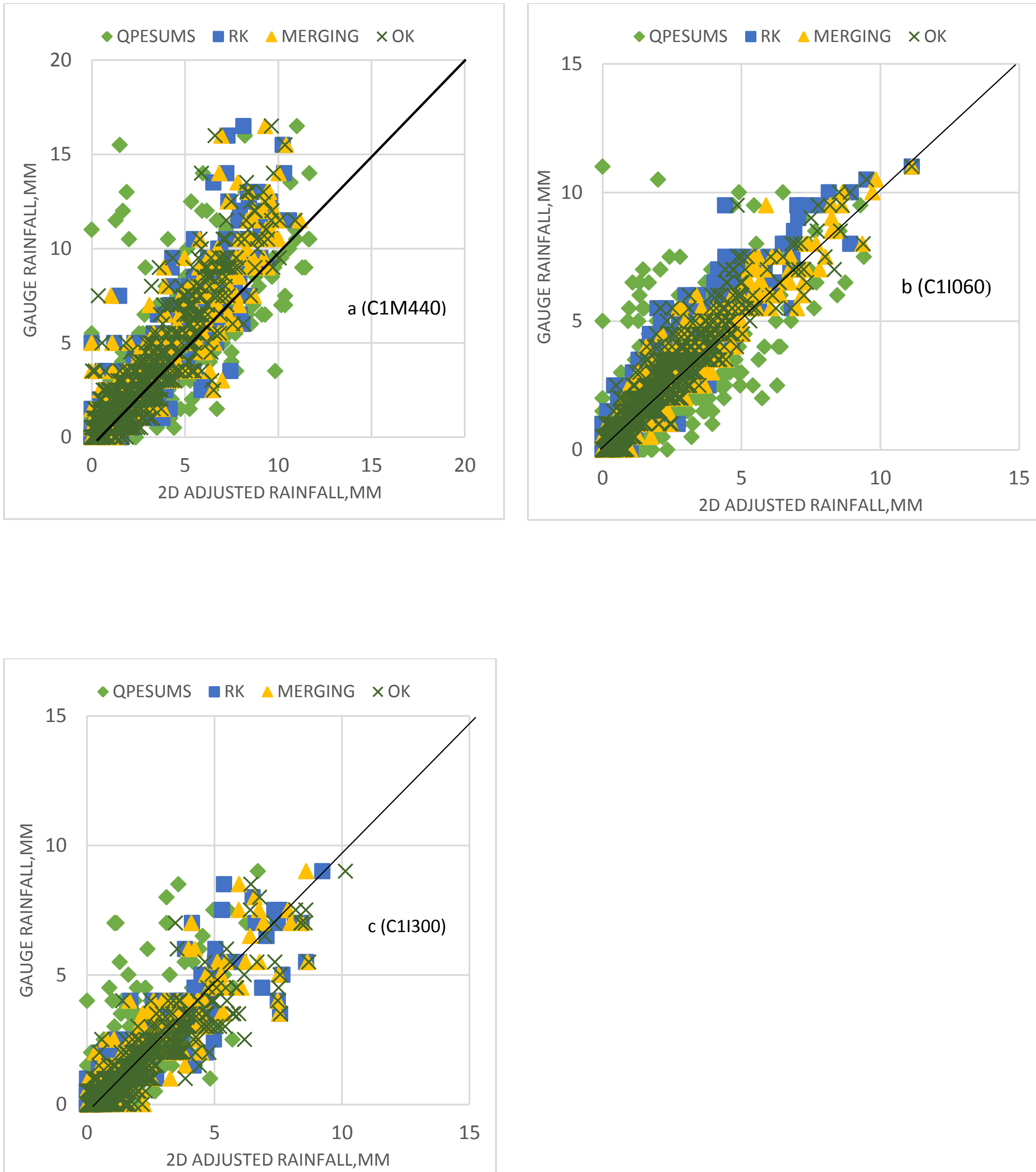

Figure 6.11. Adjusted Rainfall Rate using 2D distance versus Unadjusted Rainfall Rate obtained from Rain Gauges for typhoon Morakot

`

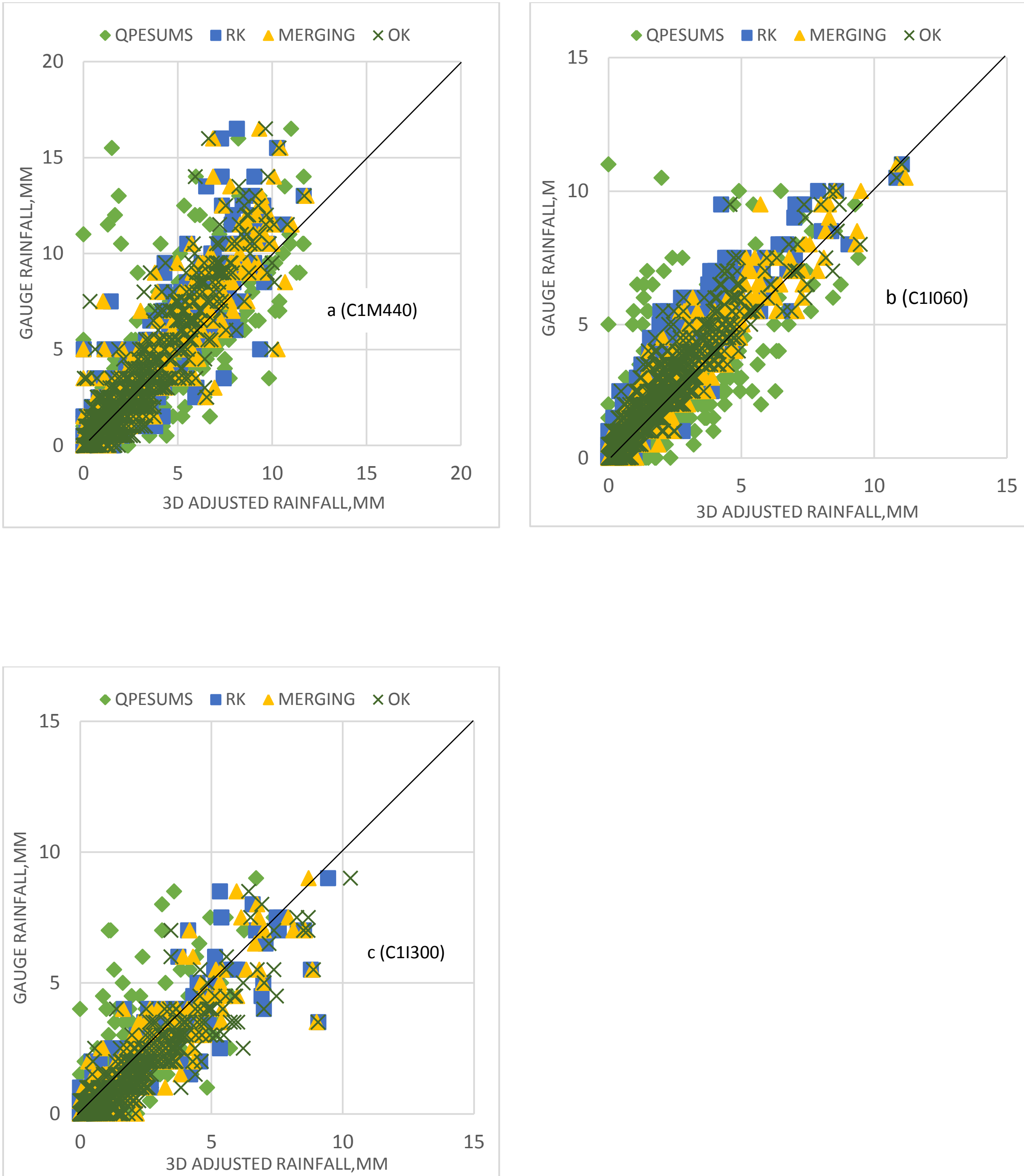

Figure 6.12. Adjusted Rainfall Rate using 3D distance versus Unadjusted Rainfall Rate obtained from Rain Gauges for typhoon Morakot

`

6.3 Typhoon Fungwong

Next, the rainfall event occurred during typhoon Fungwong is tested for the use of 2D or 3D to further comparison between interpolated distances in the calculation of adjusted radar rainfall rates using the geostatistically based RK, Merging, and OK methods. The results of RMSE analysis for the adjusted rainfall values from RK, Merging, and OK as well as the unadjusted QPESUSMS rainfall data are summarized in Table 6.3. From Table 6.3, it can be seen for the event of Typhoon Fungwong the using 3D distances is slightly less than using 2D distances for all the methods used, indicating better adjusted rainfall values are obtained using 3D distance approach. In terms of the performance of the selected methods, Merging produces better results than those from RK and OK under the case of using either 2D or 3D distances. Among the three selected stations, the results at station C1I300 are again shown to have the best rainfall estimates. The average RMSEs for the methods of RK, Merging and OK used under the condition of using 2D distances are respectively 0.9197, 0.9174, and 0.9225. However, the corresponding RMSE values for RK, Merging and OK methods using 3D distances are 0.9115, 0.9110 and 0.9186, respectively while the RMSE of unadjusted QPESUMS data, 1.8661 is about, almost double of the error of the adjusted rainfall values. Figures 6.13(a) – 6.13(c) show the percentage of improvement plot for the results using either 2D or 3D distances in the calculation by RK, Merging and OK methods. The differences between the percentage of improvement made using 2D distances and that using 3D distances are shown in Figure 6.14. It can be concluded from Figure 6.13(a) – 6.13(c) that, the adjusted rainfall rates obtained from either 2D or 3D distance based RK, Merging, and OK methods produce similar results, ranging between 40-70 percent. It is interesting to note

`

from Figure 6.14 that the rainfall adjustments made at stations C1I150, C1I160, C1I310 and 1510P088 are substantially improved when the 3D distances are used instead of 2D distances in the interpolation calculation.

In addition to show the RMSE results time series plots illustrating the comparison between the adjusted rainfall values from the methods of RK, Merging, and OK, the unadjusted rainfall values from QPESUMS, and gauge data are presented in Figures 6.15(a), 6.15(b), and 6.15(c) using 2D distances and Figures 6.16(a), 6.16(b), and 6.16(c) under the cases of applying 3D distances between rain gauges. The plots are limited to the time frame close to the time of peak. Again the QPESUMS data can be reasonably corrected by using the methods of RK, Merging, or OK and by inputting either 2D or 3D distances. The results from using 3D distances are shown to be slightly better than those obtained based on the inputs of 2D distances.

`

Table 6.3. RMSE analysis based on RK, Merging and OK by using 2D and 3D distance for Typhoon Fungwong

STATION ID	Elevation (m)	QPESUMS (mm)	RK					MERGING					OK				
			2D		3D		2D -3D	2D		3D		2D -3D	2D		3D		2D -3D
			(mm)	impr %	(mm)	impr %		(mm)	impr %	(mm)	impr %		(mm)	impr %	(mm)	impr %	
C1I270	593	1.4634	0.5483	62.5329	0.5478	62.5668	-0.0339	0.5742	60.7623	0.5865	59.9203	0.8420	0.5764	60.6155	0.5900	59.6817	0.9338
C1I150	393	1.5936	0.7080	55.5736	0.6417	59.7327	-4.1591	0.7706	51.6437	0.7266	54.4051	-2.7614	0.7232	54.6146	0.6768	57.5280	-2.9134
C1I160	399	1.5442	0.5665	63.3127	0.4731	69.3631	-6.0504	0.5441	64.7684	0.4935	68.0453	-3.2768	0.5443	64.7518	0.4952	67.9296	-3.1778
C1I310	1001	1.6237	0.7417	54.3225	0.6377	60.7262	-6.4037	0.6955	57.1668	0.5765	64.4970	-7.3302	0.6927	57.3348	0.5736	64.6749	-7.3401
C1I300	781	1.5118	0.4934	67.3649	0.5419	64.1545	3.2105	0.5107	66.2166	0.5648	62.6403	3.5764	0.4989	67.0024	0.5603	62.9408	4.0616
C0I090	878	1.7432	0.7365	57.7471	0.7539	56.7497	0.9974	0.8512	51.1683	0.8671	50.2551	0.9132	0.7274	58.2721	0.7502	56.9645	1.3075
C1I100	1771	1.6998	0.8121	52.2196	0.8050	52.6411	-0.4215	0.8683	48.9176	0.8601	49.3988	-0.4812	0.8170	51.9319	0.8108	52.2965	-0.3645
C1I120	1528	0.8884	0.7662	13.7546	0.8048	9.4025	4.3521	0.8240	7.2512	0.8553	3.7183	3.5330	0.8391	5.5463	0.8698	2.0858	3.4605
C1I290	1151	1.4641	0.6156	57.9549	0.6392	56.3446	1.6103	0.5234	64.2497	0.5163	64.7394	-0.4897	0.5222	64.3331	0.5189	64.5576	-0.2246
C1I080	536	1.5468	0.5302	65.7230	0.5366	65.3111	0.4120	0.5572	63.9780	0.5714	63.0600	0.9180	0.5378	65.2298	0.5527	64.2672	0.9626
C1I060	1181	2.0301	0.5695	71.9486	0.5516	72.8290	-0.8803	0.5857	71.1492	0.5727	71.7887	-0.6395	0.5597	72.4272	0.5386	73.4688	-1.0416
C1I070	825	1.5190	0.6521	57.0716	0.6820	55.1035	1.9681	0.5326	64.9341	0.5533	63.5770	1.3570	1.0102	33.4955	1.0213	32.7629	0.7326
C1I340	897	1.7176	0.5377	68.6953	0.5478	68.1071	0.5882	0.5334	68.9470	0.5348	68.8640	0.0830	0.5256	69.3998	0.5291	69.1937	0.2061
C1I350	887	1.7523	0.6451	63.1867	0.6479	63.0261	0.1607	0.6423	63.3467	0.6373	63.6289	-0.2821	0.6398	63.4849	0.6350	63.7599	-0.2751
C0H9A0	1595	2.4735	1.0522	57.4615	1.1054	55.3085	2.1530	0.4228	82.9053	0.4882	80.2639	2.6414	1.1346	54.1301	1.2813	48.1976	5.9325
C1V460	1949	2.8420	1.7581	38.1395	1.7403	38.7641	-0.6246	1.9545	31.2256	1.9346	31.9280	-0.7024	1.6370	42.3977	1.6120	43.2802	-0.8825
C1M440	2540	NA	NA	NA	NA	NA	NA	NA	NA	NA	NA	NA	NA	NA	NA	NA	NA
C1V170	3690	2.2610	1.0977	51.4510	1.0914	51.7293	-0.2783	1.0454	53.7639	1.0335	54.2913	-0.5273	1.0906	51.7630	1.0805	52.2087	-0.4456
C1M630	1052	2.5203	1.0969	56.4754	1.0456	58.5135	-2.0381	1.3130	47.9037	1.2669	49.7339	-1.8302	1.0743	57.3757	1.0230	59.4098	-2.0341
X467550	3845	2.4130	0.8698	63.9555	0.9165	62.0198	1.9357	0.9358	61.2197	0.9644	60.0321	1.1876	0.8437	65.0342	0.8711	63.9003	1.1339
X467530	2413	3.9832	2.7860	30.0563	2.7584	30.7479	-0.6916	2.8718	27.9009	2.8316	28.9124	-1.0114	2.8981	27.2418	2.8557	28.3073	-1.0654
C1I170	235	1.8692	0.8255	55.8366	0.8450	54.7915	1.0451	1.0286	44.9726	1.0534	43.6460	1.3266	0.8243	55.9027	0.8512	54.4636	1.4391
C1I040	1693	1.4027	0.6095	56.5449	0.6065	56.7593	-0.2144	0.6172	55.9976	0.6107	56.4606	-0.4630	0.6066	56.7522	0.5990	57.2927	-0.5405
X1510P088	1666	1.9939	1.2211	38.7599	1.1044	44.6105	-5.8506	1.1436	42.6462	1.0414	47.7723	-5.1261	1.1629	41.6789	1.0582	46.9262	-5.2473
X1510P087	2200	2.0226	0.6224	69.2293	0.6027	70.2021	-0.9728	0.5419	73.2088	0.5350	73.5487	-0.3399	0.5377	73.4176	0.5260	73.9935	-0.5759
X1510P030	1135	1.8473	1.0264	44.4396	1.0328	44.0906	0.3491	0.9954	46.1149	1.0052	45.5858	0.5290	0.9922	46.2864	1.0018	45.7701	0.5163
X1730P132	2540	2.3061	1.3644	40.8345	1.3496	41.4765	-0.6420	1.4581	36.7715	1.4209	38.3852	-1.6137	1.4075	38.9662	1.3686	40.6524	-1.6862
AVERAGE		1.9243	0.9197		0.9115			0.9174		0.9110			0.9225		0.9186		

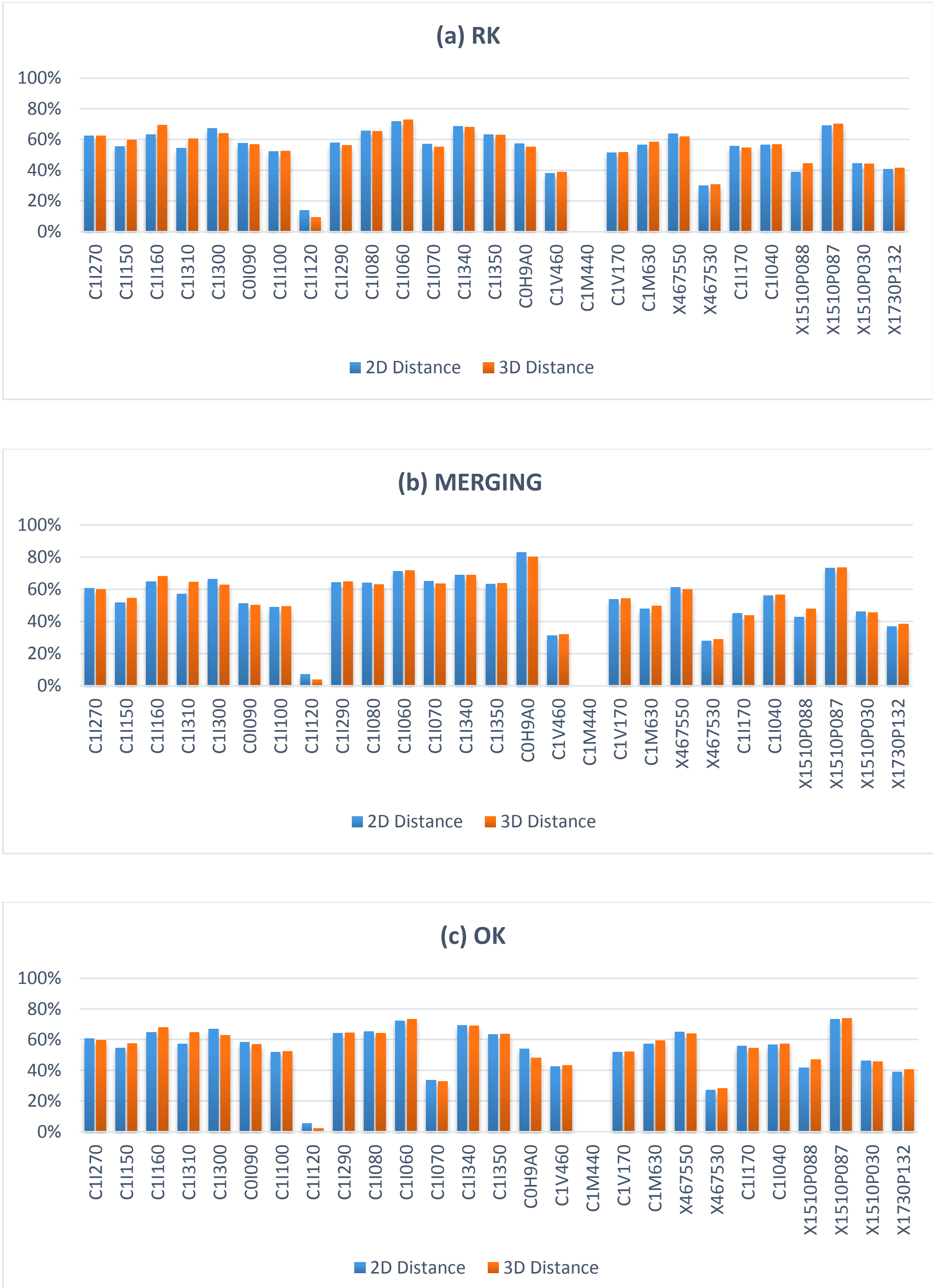

Figure 6.13. Improvements by RK, Merging and OK by 2D and 3D distance for Typhoon Fungwong

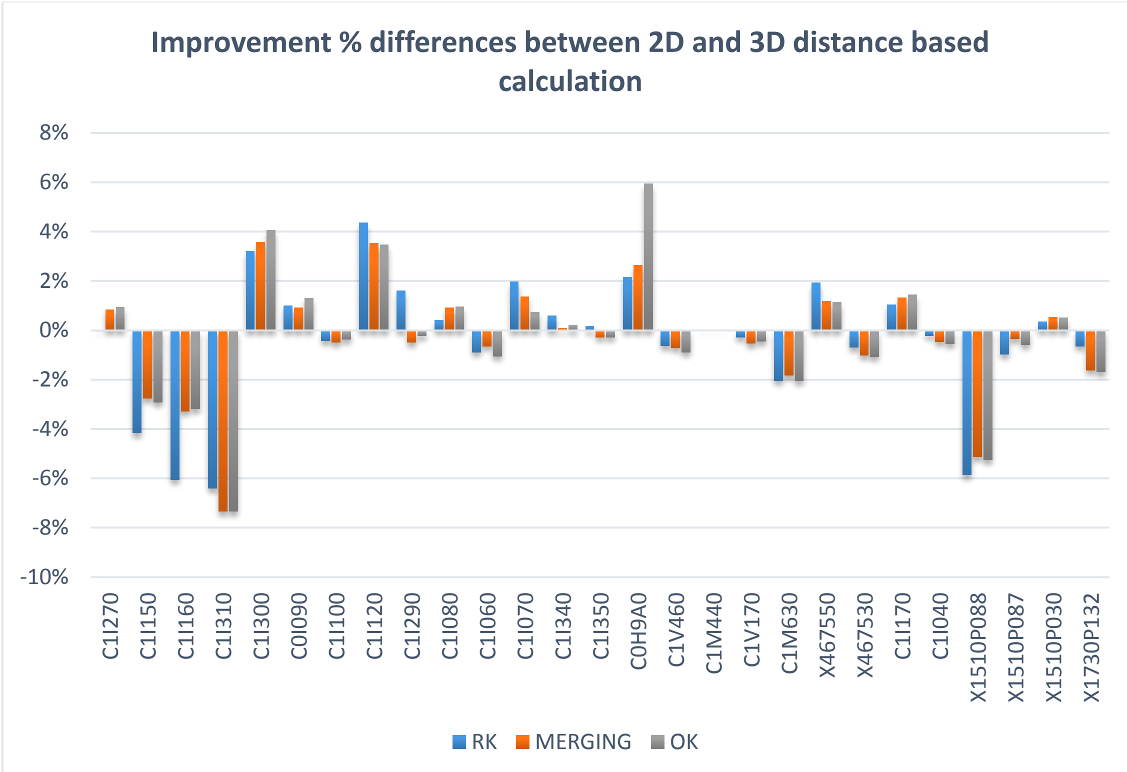

Figure 6.14. Improvement differences between 2D and 3D rain gauge distance for Typhoon Fungwong

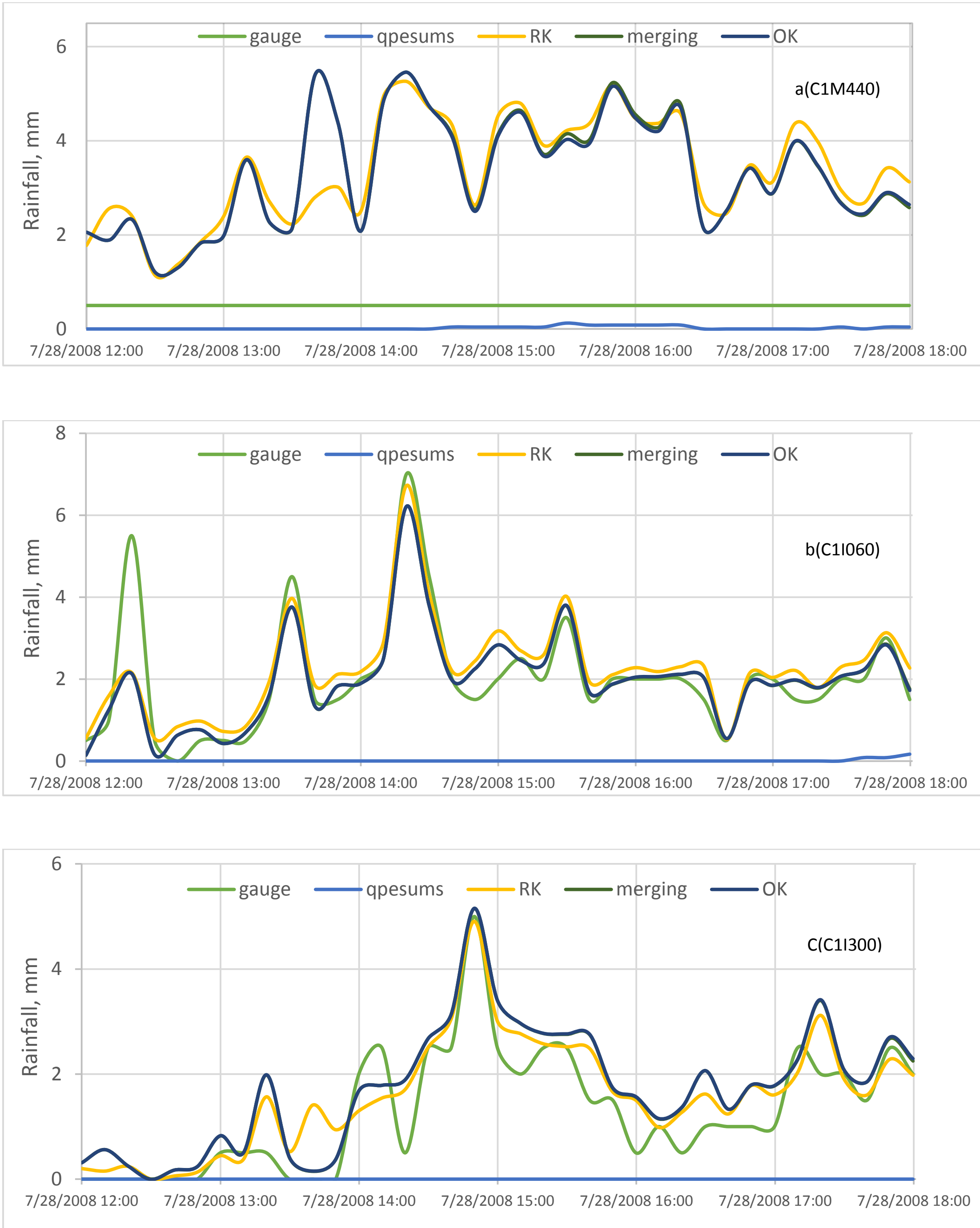

Figure 6.15. Peak hour comparison by using 2D distance for Typhoon Fungwong

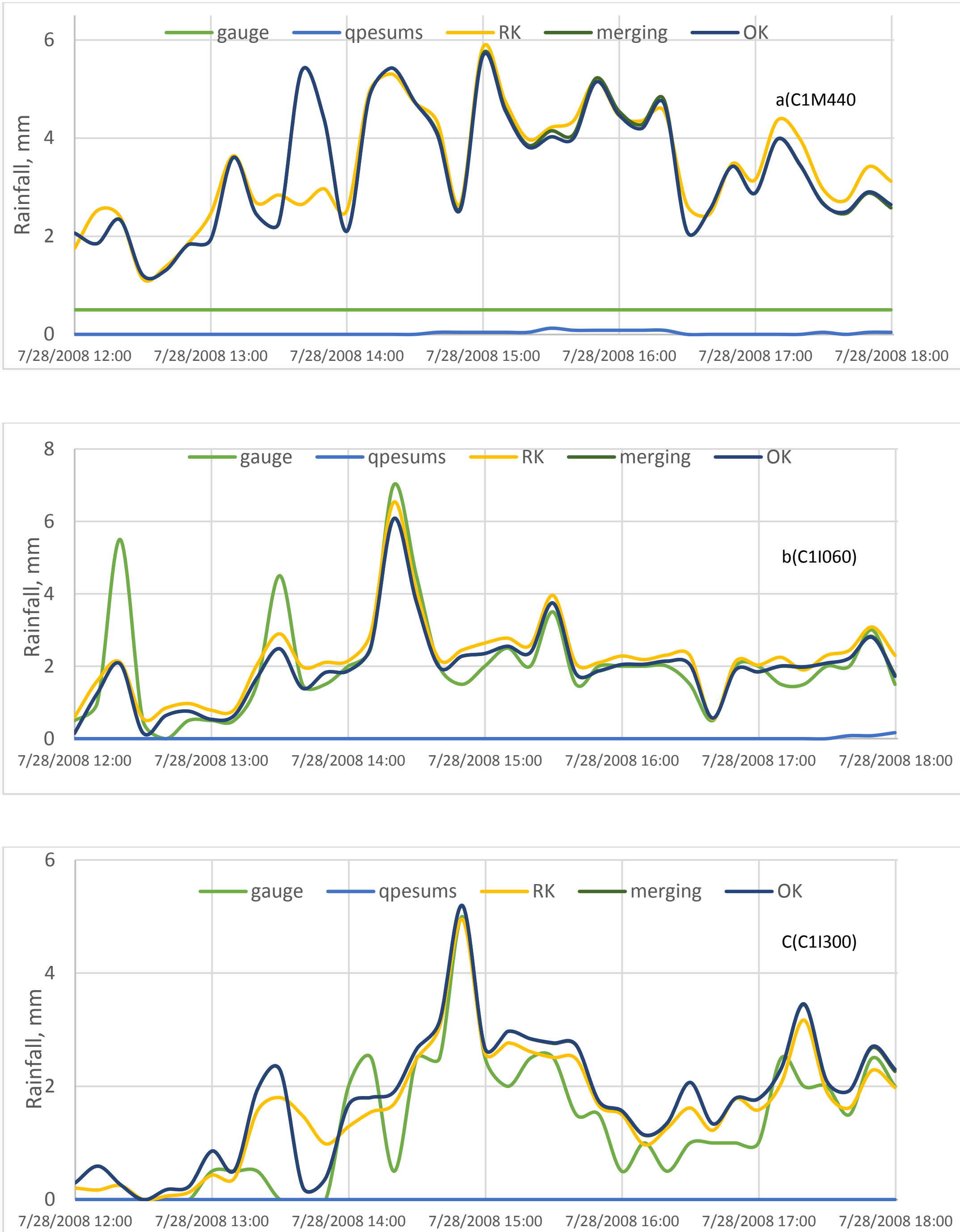

Figure 6.16. Peak hour comparison by using 3D distance for Typhoon Fungwong

6.4 Typhoon Sinlaku and Typhoon Fanapi

Similar to the rainfall adjustment studies as described above for the three typhoon events, the estimated errors in terms of RMSE for the adjusted radar rainfall values obtained from either 2D distance or 3D distance based RK, Merging, and OK methods are presented in Tables 6.4 and 6.5 respectively for the events of Typhoon Sinlaku and Typhoon Fanapi. Generally, is most gauge stations, the adjustment procedure with 3D distance based semivariogram produces better agreed rainfall values than the 2D distance based approach does. Especially, for Typhoon Fanapi, all methods (RK, Merging, and OK) using 3D distances are shown to have better adjusted rainfall values when compared to the approaches using 2D distances. Similar conclusions are reflected by the results of percentage of improvement for the adjusted rainfall values under Typhoon Sinlaku and Typhoon Fanapi are shown in Figures 6.17 and 6.18, respectively. The selected time variations of adjusted rainfall values obtained from RK, Merging, and OK methods for the event of Typhoon Sinlaku are illustrated in Figure 6.19 with the results using 2D distances and Figure 6.20 with the inputs of 3D distances. As comparisons the original QPESUMS values and gauge data are also include in Figures 6.19 and 6.20.

Table 6.4. RMSE analysis based on RK, Merging and OK by using 2D and 3D distance for Typhoon Sinlaku

STATION ID	Elevation (m)	QPESUMS (mm)	RK					MERGING					OK				
			2D		3D		2D -3D	2D		3D		2D -3D	2D		3D		2D -3D
			(mm)	impr %	(mm)	impr %		(mm)	impr %	(mm)	impr %		(mm)	impr %	(mm)	impr %	
C1I270	593	1.2216	0.9625	21.2149	0.9566	21.6911	-0.4761	0.9477	22.4190	0.9472	22.4600	-0.0409	1.0797	11.6171	1.0794	11.6445	-0.0274
C1I150	393	1.0601	0.9108	14.0841	0.9043	14.6941	-0.6100	0.8967	15.4103	0.8981	15.2831	0.1272	1.0952	-3.3185	1.0946	-3.2575	-0.0609
C1I160	399	0.9347	0.6138	34.3340	0.6094	34.8043	-0.4703	0.6200	33.6710	0.6200	33.6622	0.0088	0.7451	20.2806	0.7460	20.1841	0.0965
C1I310	1001	0.9650	0.6001	37.8149	0.5952	38.3227	-0.5078	0.5779	40.1119	0.5775	40.1548	-0.0429	0.6416	33.5115	0.6411	33.5594	-0.0479
C1I300	781	0.8429	0.6280	25.5026	0.6233	26.0536	-0.5510	0.6037	28.3782	0.6001	28.8095	-0.4313	0.6622	21.4432	0.6598	21.7275	-0.2843
C0I090	878	1.0221	0.9109	10.8778	0.9030	11.6465	-0.7687	0.8649	15.3806	0.8649	15.3799	0.0007	1.0465	-2.3918	1.0458	-2.3258	-0.0660
C1I100	1771	NA	NA	NA	NA	NA	NA	NA	NA	NA	NA	NA	NA	NA	NA	NA	NA
C1I120	1528	0.8534	1.4748	-72.8198	1.4604	-71.1240	-1.6958	0.8503	0.3662	0.8522	0.1407	0.2255	1.0633	-24.5977	1.0644	-24.7203	0.1226
C1I290	1151	0.8737	0.8691	0.5307	0.8588	1.7089	-1.1782	0.6330	27.5497	0.6293	27.9713	-0.4215	0.7033	19.5038	0.6993	19.9680	-0.4642
C1I080	536	0.9182	0.8187	10.8322	0.8083	11.9666	-1.1343	0.6860	25.2905	0.6844	25.4585	-0.1680	0.8652	5.7729	0.8595	6.3986	-0.6257
C1I060	1181	1.1432	0.8700	23.9012	0.9041	20.9199	2.9813	0.6860	39.9949	0.7061	38.2392	1.7557	0.8212	28.1690	0.8679	24.0837	4.0854
C1I070	825	0.9762	0.8725	10.6282	0.8652	11.3702	-0.7420	0.8670	11.1897	0.8643	11.4605	-0.2708	0.8740	10.4672	0.8734	10.5280	-0.0608
C1I340	897	0.9941	1.0037	-0.9717	0.9959	-0.1856	-0.7861	0.8651	12.9760	0.8647	13.0150	-0.0390	0.8903	10.4326	0.8893	10.5339	-0.1013
C1I350	887	0.8391	0.7872	6.1859	0.7823	6.7749	-0.5890	0.7884	6.0456	0.7898	5.8760	0.1697	0.8170	2.6306	0.8173	2.5990	0.0316
C0H9A0	1595	1.0979	1.0175	7.3222	1.0079	8.2014	-0.8792	0.8640	21.3050	0.8608	21.5961	-0.2911	0.9405	14.3362	0.9375	14.6107	-0.2746
C1V460	1949	1.0058	0.9530	5.2496	0.9465	5.8966	-0.6470	0.9662	3.9399	0.9650	4.0538	-0.1139	1.1268	-12.0360	1.1241	-11.7680	-0.2679
C1M440	2540	0.9993	0.8058	19.3598	0.8195	17.9936	1.3662	0.8115	18.7962	0.8358	16.3630	2.4332	0.8793	12.0104	0.8972	10.2147	1.7956
C1V170	3690	0.8808	0.7934	9.9221	0.7963	9.5913	0.3308	0.8554	2.8881	0.8660	1.6751	1.2131	1.0013	-13.6758	1.0106	-14.7376	1.0618
C1M630	1052	1.2702	2.3866	-87.8982	2.3683	-86.4528	-1.4455	1.2547	1.2199	1.2554	1.1610	0.0589	2.0070	-58.0141	2.0081	-58.0990	0.0849
X467550	3845	1.1368	0.9791	13.8664	0.9711	14.5784	-0.7120	0.9548	16.0037	0.9574	15.7810	0.2227	1.1068	2.6398	1.1071	2.6115	0.0283
X467530	2413	1.6452	1.4077	14.4361	1.3938	15.2806	-0.8446	1.3555	17.6118	1.3514	17.8615	-0.2498	1.5268	7.1968	1.5235	7.3968	-0.2000
C1I170	235	1.1468	1.0809	5.7478	1.0737	6.3689	-0.6211	1.0694	6.7497	1.0685	6.8257	-0.0760	1.2036	-4.9536	1.2023	-4.8444	-0.1093
C1I040	1693	1.1370	1.1826	-4.0068	1.1771	-3.5276	-0.4791	1.2231	-7.5675	1.2247	-7.7052	0.1377	1.8217	-60.2105	1.8224	-60.2784	0.0679
X1510P088	1666	0.9870	0.9371	5.0481	0.9303	5.7419	-0.6938	0.7784	21.1347	0.7777	21.2014	-0.0668	0.8014	18.8012	0.8075	18.1813	0.6199
X1510P087	2200	1.1567	0.6874	40.5696	0.7124	38.4152	2.1544	0.6564	43.2567	0.6726	41.8489	1.4078	0.7350	36.4577	0.7732	33.1569	3.3008
X1510P030	1135	1.1957	1.1840	0.9827	1.1765	1.6087	-0.6260	1.1042	7.6515	1.1052	7.5746	0.0769	1.1177	6.5232	1.1188	6.4336	0.0896
X1730P132	2540	1.2026	0.9319	22.5154	0.9322	22.4854	0.0300	0.9406	21.7847	0.9524	20.8102	0.9745	0.9225	23.2905	0.9340	22.3347	0.9558
AVERAGE		1.0396	1.0116		1.0078			0.8684		0.8711			1.0347		1.0390		

Table 6.5. RMSE analysis based on RK, Merge and OK by using 2D and 3D distance for Typhoon Fanapi

STATION ID	Elevation (m)	QPESUMS (mm)	RK					MERGING					OK				
			2D		3D		2D -3D	2D		3D		2D -3D	2D		3D		2D -3D
			(mm)	impr %	(mm)	impr %		(mm)	impr %	(mm)	impr %		(mm)	impr %	(mm)	impr %	
C1I270	593	0.7584	0.4872	35.7628	0.5028	33.7024	2.0605	0.6180	18.5125	0.6327	16.5739	1.9386	0.5416	28.5850	0.5396	28.8512	-0.2663
C1I150	393	0.9556	0.4390	54.0644	0.4478	53.1440	0.9205	0.5507	42.3735	0.5743	39.9050	2.4686	0.5458	42.8873	0.5385	43.6486	-0.7613
C1I160	399	0.6167	0.5147	16.5346	0.5460	11.4586	5.0761	0.6788	-10.0704	0.6988	-13.3257	3.2553	0.5726	7.1404	0.5911	4.1434	2.9970
C1I310	1001	0.9835	0.4115	58.1605	0.4101	58.3024	-0.1419	0.4214	57.1528	0.4188	57.4219	-0.2691	0.5037	48.7906	0.5048	48.6743	0.1163
C1I300	781	0.7506	0.5238	30.2227	0.5321	29.1159	1.1068	0.6311	15.9272	0.6370	15.1432	0.7840	0.5324	29.0674	0.5370	28.4597	0.6077
C0I090	878	0.9080	0.5446	40.0168	0.5766	36.5002	3.5166	0.6446	29.0046	0.6658	26.6762	2.3284	0.6087	32.9582	0.6225	31.4406	1.5176
C1I100	1771	1.1955	0.4447	62.8059	0.4384	63.3262	-0.5203	0.5026	57.9584	0.4906	58.9636	-1.0052	0.6499	45.6401	0.6416	46.3294	-0.6893
C1I120	1528	0.7158	0.6096	14.8382	0.6397	10.6301	4.2081	0.6829	4.5881	0.7119	0.5467	4.0414	0.6238	12.8443	0.6451	9.8783	2.9660
C1I290	1151	1.5176	0.5496	63.7839	0.5622	62.9525	0.8315	0.5567	63.3152	0.5553	63.4113	-0.0961	0.6877	54.6844	0.6660	56.1156	-1.4312
C1I080	536	1.2670	0.6692	47.1825	0.6640	47.5938	-0.4113	0.6936	45.2550	0.6881	45.6898	-0.4348	0.7882	37.7872	0.7790	38.5161	-0.7289
C1I060	1181	3.8061	1.8384	51.6992	1.1819	68.9463	-17.2470	1.9461	48.8702	1.3308	65.0362	-16.1660	2.1881	42.5120	1.6265	57.2674	-14.7554
C1I070	825	1.6700	0.8622	48.3690	1.0535	36.9154	11.4536	0.7289	56.3553	0.9355	43.9806	12.3747	0.7054	57.7580	0.8363	49.9236	7.8344
C1I340	897	1.0060	0.4723	53.0512	0.4485	55.4223	-2.3712	0.4349	56.7751	0.4230	57.9588	-1.1837	0.7558	24.8764	0.7736	23.1024	1.7739
C1I350	887	1.5411	0.4855	68.4941	0.4939	67.9541	0.5400	0.4005	74.0105	0.4131	73.1929	0.8176	0.7224	53.1282	0.7247	52.9735	0.1547
C0H9A0	1595	1.3611	0.5714	58.0212	0.5523	59.4180	-1.3968	0.5048	62.9114	0.4812	64.6439	-1.7325	0.7748	43.0748	0.7464	45.1615	-2.0867
C1V460	1949	2.4500	1.0953	55.2913	1.0312	57.9107	-2.6194	1.1920	51.3466	1.1195	54.3059	-2.9593	1.4431	41.0987	1.3716	44.0140	-2.9154
C1M440	2540	2.1607	1.0549	51.1766	1.0062	53.4323	-2.2557	1.1742	45.6591	1.1199	48.1714	-2.5124	1.4137	34.5730	1.3654	36.8070	-2.2340
C1V170	3690	3.0427	1.1536	62.0858	0.9790	67.8254	-5.7396	1.3126	56.8603	1.0863	64.2972	-7.4369	1.8937	37.7625	1.7300	43.1427	-5.3802
C1M630	1052	1.6942	0.7937	53.1540	0.8003	52.7638	0.3902	0.9357	44.7682	0.9403	44.4981	0.2701	0.9927	41.4080	0.9899	41.5713	-0.1633
X467550	3845	3.0983	1.0862	64.9431	0.9607	68.9916	-4.0485	1.3071	57.8132	1.1335	63.4153	-5.6022	1.7858	42.3609	1.6548	46.5883	-4.2274
X467530	2413	2.5491	1.3312	47.7757	1.3132	48.4839	-0.7083	1.5005	41.1364	1.5003	41.1441	-0.0077	1.7989	29.4288	1.7880	29.8575	-0.4287
C1I170	235	0.4007	0.5021	-25.2928	0.5372	-34.0675	8.7747	0.7345	-83.2964	0.7736	-93.0612	9.7648	0.5886	-46.8800	0.6093	-52.0428	5.1628
C1I040	1693	1.6030	0.6712	58.1313	0.6670	58.3937	-0.2624	0.7404	53.8113	0.7344	54.1889	-0.3776	0.8191	48.9010	0.7909	50.6622	-1.7612
X1510P088	1666	1.9515	1.1923	38.9026	1.1387	41.6505	-2.7479	1.0617	45.5964	1.0024	48.6353	-3.0389	1.3543	30.6021	1.3009	33.3365	-2.7344
X1510P087	2200	3.5633	1.6265	54.3538	0.8286	76.7471	-22.3933	1.5896	55.3901	0.8120	77.2112	-21.8212	1.9033	46.5860	1.2188	65.7946	-19.2087
X1510P030	1135	1.9597	0.8153	58.3947	0.8002	59.1660	-0.7713	0.6885	64.8648	0.6741	65.6037	-0.7389	1.2250	37.4895	1.2174	37.8772	-0.3876
X1730P132	2540	NA	NA	NA	NA	NA	NA	NA	NA	NA	NA	NA	NA	NA	NA	NA	NA
AVERAGE		1.6741	0.7979		0.7351			0.8551		0.7905			1.0161		0.9542		

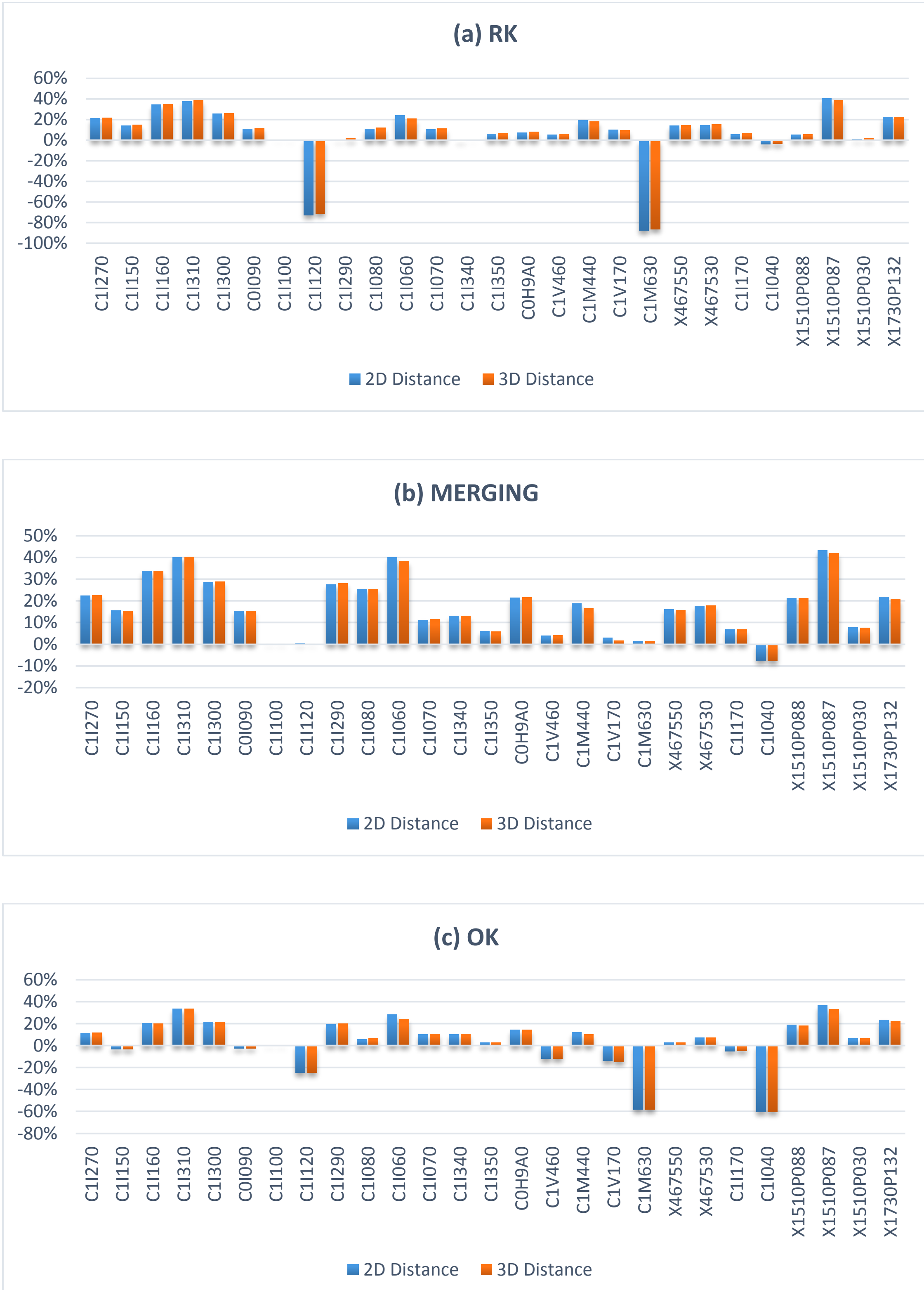

Figure 6.17. Improvements by RK, Merging and OK by 2D and 3D distance for Typhoon Sinlaku.

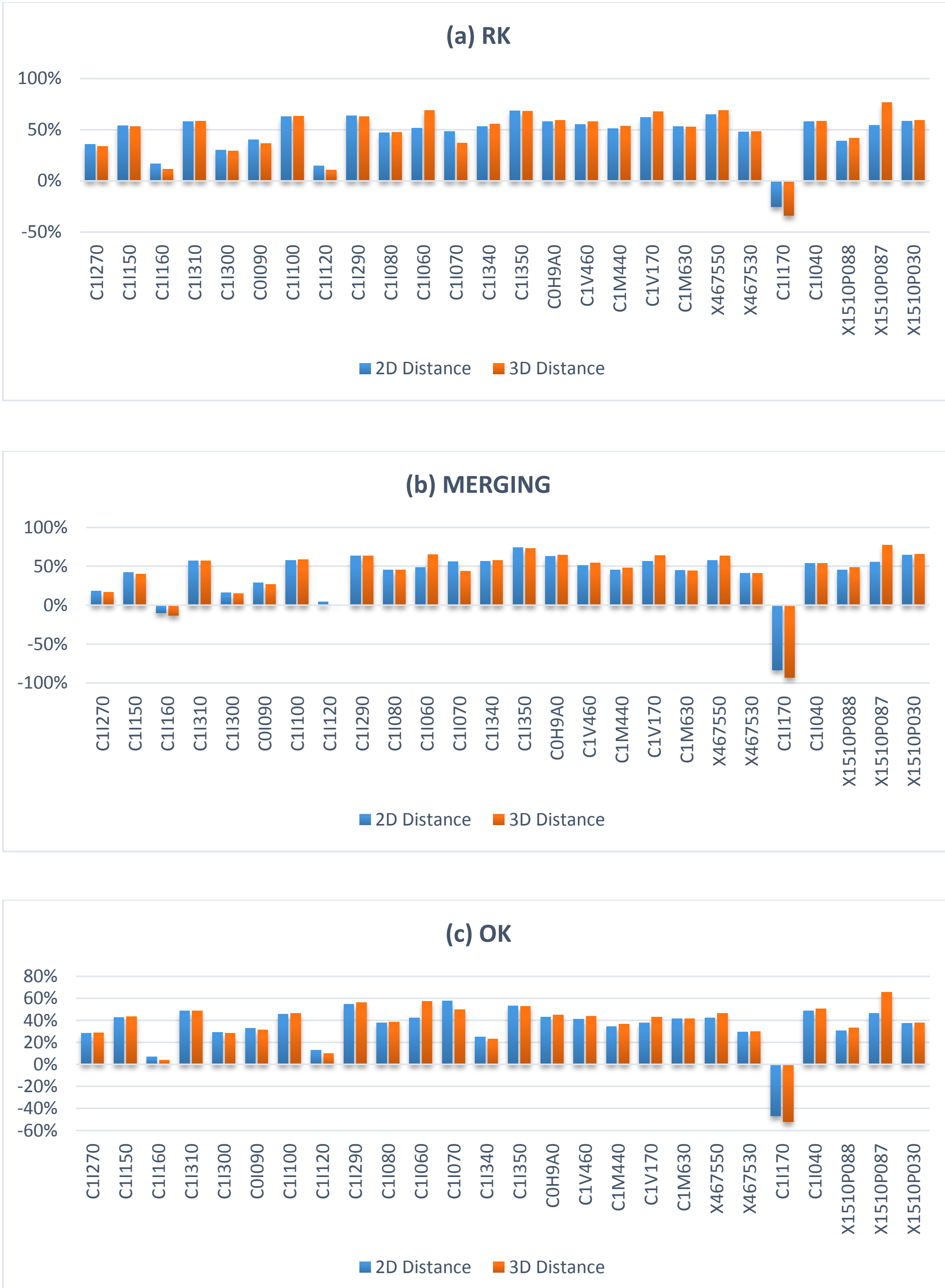

Figure 6.18. Improvements by RK, Merging and OK by 2D and 3D distance for Typhoon Fanapi

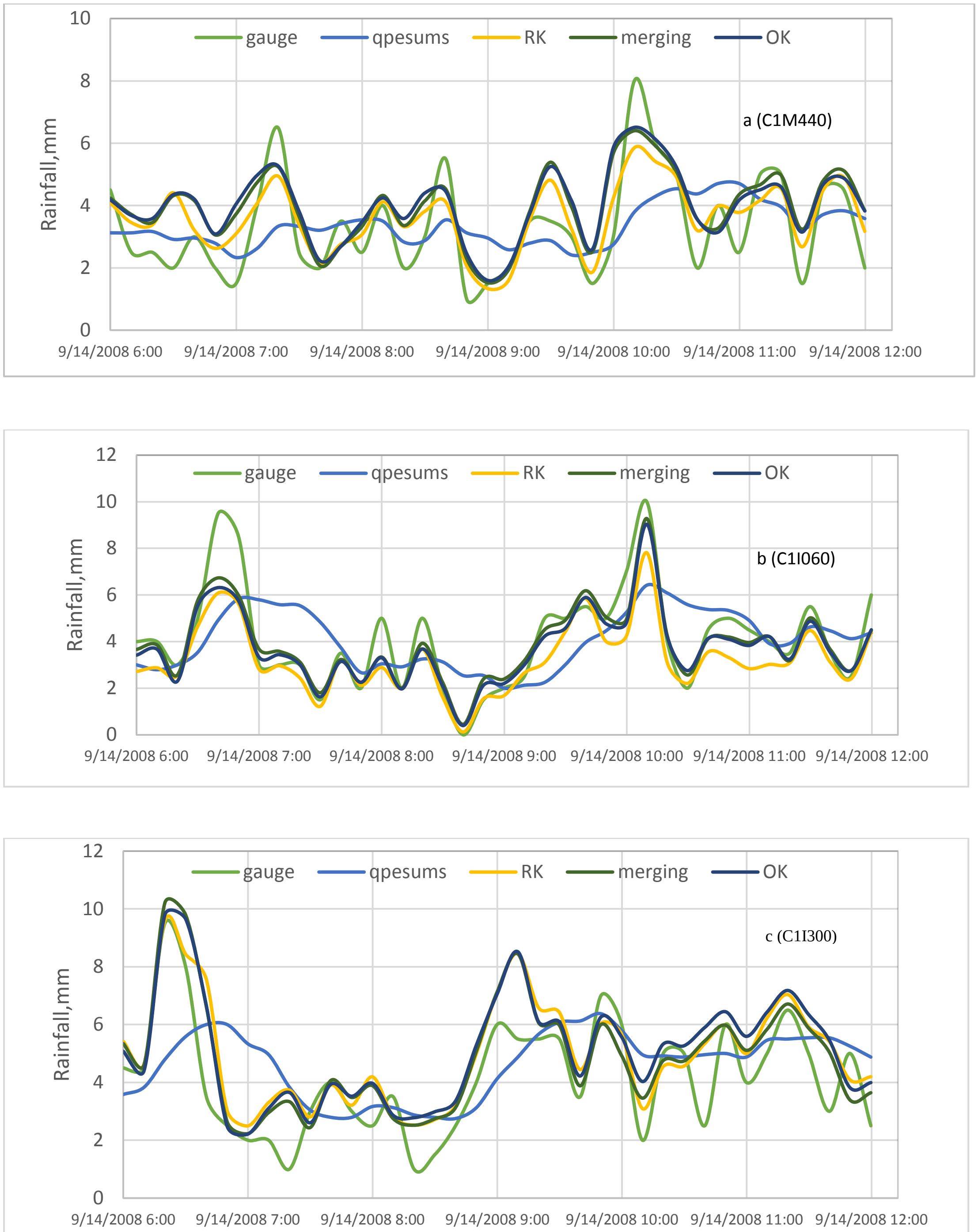

Figure 6.19. Peak hour comparison by using 2D distance for Typhoon Sinlaku

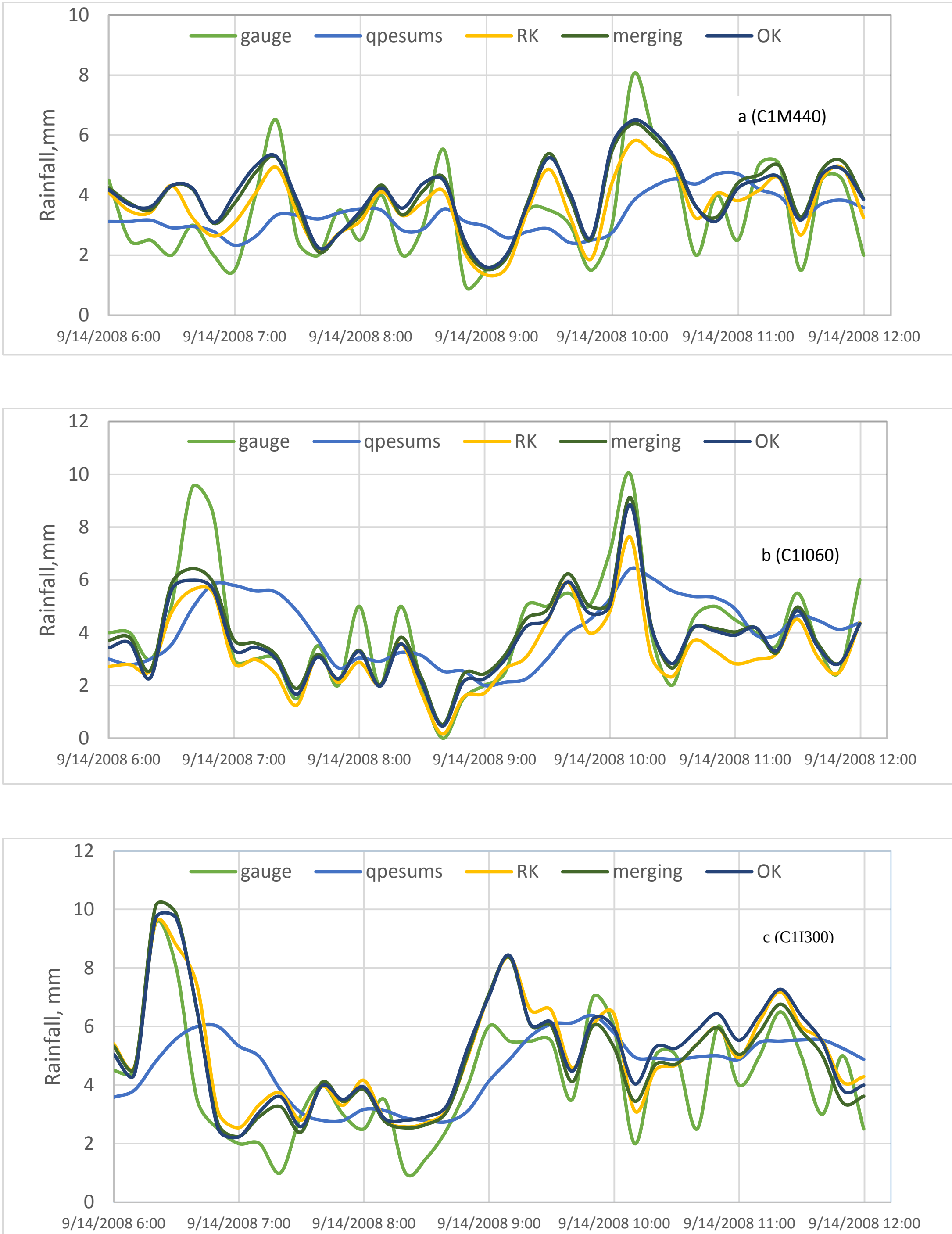

Figure 6.20. Peak hour comparison by using 3D distance for Typhoon Sinlaku

7 Conclusions and Recommendations for Future Studies

In this study the adjustments of radar rainfall rates from QPESUMS for five typhoon events at the Chenyulan river watershed in Taiwan are investigated with Regression Kriging (RK) and Merging methods. Both of these methods are multivariate methods. In addition to multivariate techniques, a univariate technique, Ordinary Kriging (OK) is also used to produce results for comparisons. The rainfall data obtained from rain gauges as target variable and weather radar as auxiliary variable are combined to improve the accuracy of rainfall estimates by utilizing the semivariogram based interpolation methods. Especially, the distances between gauge stations used for the development of the semivariograms comprise 2D distances and true 3D distances. Five historical typhoon events hit Taiwan in the past are selected to test the rainfall adjustment models, such as RK and Merging, and to examine the effect of 3D distance on the corrected rainfall values. The Typhoons include Kalmaegi (2008), Morakot (2009), Fungwong (2008), Sinlaku (2008) and Fanapi (2010). The geostatistically determined rainfall adjustments are cross validated with the rain gauge measurements. The leave one out cross validation (LOOCV) procedure is followed to perform the cross validation. As the distance based semivariogram is used to geostatistically correct the radar rainfall rates through the interpolation procedure, this study is aimed to include the 3D true distances (latitude, longtitude, elevation) instead of the commonly used 2D distances (latitude, longtitude) in the calculation and evaluate the accuracy of the results. The simulations of the five typhoon rainfall events for the adjustments of data using RK, Merging and OK models were performed and the results are compared with gauge measurements. The error analysis with the calculated root mean squared errors (RMSEs), the percentage of improvement, and the direct comparisons between adjusted and unadjusted values given in the time series and fitted with 45 degree line plots are presented for the selected three stations, C1M440, C1I060 and C1I300. The results suggest that in general the radar rainfall data can be adjusted to be more accurately by using multivariate techniques such as RK and Merging methods, than those from univariate method OK. Also, depending on the typhoon events, using 3D distances in the semivariogram and geostatistically based interpolation calculations is shown to be able to produce better estimates than using 2D distances in some of the gauge stations or, at least, similar to the results from 2D distances approach. Comparing the results of RMSEs station by station the 3D distance based approach reveal more improved results in 15 stations for RK, 13 stations for Merging, and 16 stations for OK method out of total 27 stations, especially for the stations located at high elevation for typhoon Kalmaegi. Besides, the results for Typhoon Sinlaku and Fanapi 3D distance based calculation produce better rainfall prediction than those by using 2D distance based calculation for all spatial interpolation methods, RK, Merging, and OK. Especially at the stations C1I060 and 1510P087 for the Typhoon Fanapi, using 3D distance based calculation showed around 15 % – 20 % better rainfall prediction than those 2D distance calculation.

For the future studies, it is suggested to perform the geostatistically based interpolation methods in a larger watershed but with more scattered gauge stations distribution examine the effect of the station elevation (or 3D distance) on the overall performance in adjusting the radar rainfall data. The other topics can be considered for future studies are to include the high elevation associated rainfall blockage (e.g. by trees and others) factor and the angles of radar reflectivities as additional modelling parameters to further improve the adjustment tool for radar rainfall data, especially for the watershed with high elevation terrain.

REFERENCES

Berne, A, & Krajewski, W.F. (2013). "Radar for Hydrology: Unfulfilled Promise or Unrecognized Potential?" *Advances in Water Resources* 51 (2013) 357-366.

Borga, M., (2002) "Accuracy of Rainfall Estimates for Streamflow Simulation.*" Journal of Hydrology* 267 (2002) 26-39

Chen, F.W., & Liu, C.W., (2012) "Estimation of the Spatial Rainfall Distribution Using Inverse Distance Weighting (IDW) in the Middle of Taiwan." *Paddy Water Environ.* (2012) 10:209-222

Chen, S., Hong, Y., Cao., Kirstetter, P.E., Gourley, J.J., Qi, Y., Zhang, J., Howard, K., Hu, J., & Wang, J. (2013) "Performance Evaluation of Radar and Satellitte Rainfalls for Typhoon Morakot Over Taiwan: Are Remote-Sensing Products Ready for Gauge Denial Scenario of Extreme Events?" *Journal of Hydrology* 506 (2013) 4-13

Chu, Ted. (2014) "Geostatistical Interpolation of Rain Fields Using Radar Estimates and Gauge Observation: Algorithm Design and Automation." *Doctoral Dissertation, University of Houston*

Chumchean, S., Seed, A., & Sharma, A. (2004) "Application of Scaling in Radar Reflectivity for Correcting Range-Dependent Bias in Climatological Radar Rainfall Estimates." *Journal of Atmospheric and Oceanic Technology*, Vol. 21

Chumchean, S., Seed, A., & Sharma, A. (2006) "An Integrated Approach to Error Correction for Real Time Radar Rainfall Estimation." *Journal of Atmospheric and Oceanic Technology*, Vol. 23

Chumchean, S., Seed, A., & Sharma, A. (2008) “An Operation Approach for Classifying Stroms in Real Time Radar Rainfall Estimation.” *Journal of Hydrology* (2008) 363, 1-17

Cole, S., & Moore, Robert. (2008) “Hydrological Modelling Using Raingauge and Radar-Based Estimators of Areal Rainfall.” *Journal of Hydrology* (2008) 358, 159-181

Delbari, M., & Afrasiab, P. (2013). “Spatial Interpolation of Monthly and Annual Rainfall in Northeast of Iran.” *Meteoral Atmos Phys* (2013) 122:103-113.

Delrieu, G., Wijbrans, A., Boudevillain, B., Faure. D.,Bonnifait, L., Kirstetter, P.E. (2014) “Geostatistical Radar-Raingauge Merging: A Novel Method for the Quantification of Rain Estimation Accuracy.” *Advances in Water Resources* 71 (2014) 110-124

Ehret, U. (2003) “Rainfall and Flood Nowcasting in Small Catchment Using Weather Radar” *Doctoral Dissertation, Universtiy of Stuttgart*

Forero, C.A.V., Torres, D.A., Cassiraga, E.F., & Hernandez, J.J.G (2009) “A non Parametric Automatic Blending Methodology to Estimate Rainfall Fields From Rain Gauge and Radar Data.” *Advances in Water Resources* 32 (2009) 986-1002

Gooverts, P. (2000). “Geostatistical Approaches for Incorporating Elevation Into the Spatial Interpolation of Rainfall.” *Journal of Hydrology* 228 (2000) 113-129.

Goudenhoofdt, E., & Delobbe, L., (2009) “Evaluation of Radar-Gauge Merging Methods for Quantitative Precipitation Estimates.” *Hydrology and Earth System Sciences* 13, 195-203, 2009

Hanchoowong, R., Weesakul, U., & Chumchean, S. (2012). "Bias Correction of Radar Rainfall Estimates Based on a Geostatistical Technique." *ScienceAsia* 38 (2012) 373-385

Hengl, T., Heuvelink, G.B.M., & Stein, A. (2004) "A Generic Framework for Spatial Prediction of Soil Variables Based on Regression Kriging." *Geoderma* 120 (2004) 75-93

Joss, J., & Lee, R. (1995) "The Application of Radar-Gauge Comparison to Operational Precipitation Profile Corrections." *Journal of Applied Meterology*, Vol. 34

Knight, Y., Yu, B., Jenkins, G., & Morris (2005) "Comparing Rainfall Interpolation Techniques for Small Subtropical Urban Catchments." *Modelling and Simulation Society of Australia and New Zealand, Conference Publication* (2005)

Lopez, V., Napolitano, F., & Russo, F. (2005) "Calibration of a Rainfall-Runoff Model Using Radar and Raingauge." Advances in Geosciences, 2, 41-46, 2005

Prudhomme, C., Reed, D.W. (1999) "Mapping Extreme Rainfall in a Mountainous Region Using Geostatistical Techniques: A Case Study in Scotland." International Journal of Climatology, 19: 1337-1356(1999)

R Core Team. (2013). *R: a Language and Environment for Statistical Computing*. Vienna, Austria: R Foundation for Statistical Computing.

Roger, A., Pielke, JR., Downton, M. (2000). "Precipitation and Damaging Floods: Trends in the United States, 1932-97." *Journal of Climate*, Vol.13

Sarangi, A., Cox, C.A., & Madramootoo, C.A. (2005) "Geostatistical Methods For Prediction of Spatial Variability of Rainfall in a Mountainous Region." *American Society of Agricultural Engineers* ISSN 0001-2351, Vol.48 (3):943-954

Sun, W., Minasny, B., & McBratney, A. (2012) “Analysis and Prediction of Soil Properties Using Local Regression Kriging.” *Geoderma* 171-172 (2012) 16-23

Tabios, G. & Salas, J.D. (1985) “A Comparative Analysis of Techniques for Spatial Interpolation of Precipitation.” *Water Resources Bulletin American Water Resources Association* Vol.21, No.3

Teng, H., Shi, Z., Ma, Z., & Li, Y. (2014) “Estimating Spatially Downscaled Rainfall by Regression Kriging Using TRMM Precipitation and Elevation in Zhejiang Province, Southeast China.” *International Journal of Remote Sensing* Vol. 35, No. 22, 7775-7794

Wardah, T., Sharifah Nurul Huda, S.Y., Deni, S.M., & Nur Azwa, B. (2011) “Radar Rainfall Estimates Comparison with Kriging Interpolation of Gauged Rain.*” IEEE Colloquium on Humanities, Science and Engineering Research (CHUSER 2011)*